3 Biotech (2019) 9:185
https://doi.org/10.1007/s13205-019-1720-x

ORIGINAL ARTICLE

Modeling a pH-sensitive Zein-*co*-acrylic acid hybrid hydrogels loaded 5-fluorouracil and rutin for enhanced anticancer efficacy by oral delivery

Selvaraj Kunjiappan[1] · Panneerselvam Theivendran[2] · Suraj Baskararaj[1] · Bathrinath Sankaranarayanan[3] · Ponnusamy Palanisamy[4] · Govindaraj Saravanan[5] · Sankarganesh Arunachalam[1] · Murugesan Sankaranarayanan[6] · Jawahar Natarajan[7] · Balasubramanian Somasundaram[1] · Ashish Wadhwani[8]

Received: 7 June 2018 / Accepted: 17 April 2019 / Published online: 23 April 2019

Abstract

The combination of natural and synthetic polymeric materials grafted hydrogels offer great potential as oral therapeutic systems because of its intrinsic biocompatibility, biodegradability, protect labile drugs from metabolism and controlled release properties. Hence, in the present study, we aimed to prepare and optimize oral delivered pH-responsive Zein-*co*-acrylic acid hydrogels incorporated with 5-fluorouracil (5-Fu) and rutin (Ru) for effective anticancer activity with less toxicity. In this study, graft polymerization technique is adopted to formulate hydrogels with various ratios of Zein, acrylic acid, *N*, *N*-methylene bisacrylamide, and ammonium persulphate as an initiator. The optimized formulation was identified based on the cross-linking, chemical interactions, intrinsic viscosity (η), dynamic swelling (Q) at pH 1.2, diffusion coefficient (D), sol–gel fraction (%), and porosity (%). The selected optimized formulation has shown significant improvement in drugs loading and encapsulation efficiency, releasing at pH 1.2 and pH 7.4. Drug release kinetics studies confirmed the controlled release properties of hydrogels. Hydrogels were porous and the drug loading of 5-Fu and Ru was found to be 12.13% and 10.86%, respectively, whereas encapsulation efficiency of 5-Fu and Ru was 89.35% and 81.47%, respectively. Furthermore, form the in vitro cytotoxic screening, it was found that 52.5 μg mL^{-1} 5-Fu and Ru-loaded hydrogel impacted 50% of cell death at 24 h, there by significantly arresting the proliferation of MDA-MB-231 and MCF-7 breast cancer cell lines. Altogether, the optimized pH-responsive hydrogels make them favorable carrier for anticancer drugs for oral delivery.

Keywords Hydrogel · Drug delivery system · Anticancer activity · 5-fluorouracil · Rutin

Introduction

As a disease, cancer is a complicated phenomenon that necessitates high-throughput research. Understanding cancer progression in humans is not correctly adaptable through animal models. However, recent trends have shown that hydrogel-based reconstructive models could improve the therapeutic efficacy and can properly simulate the tumor microenvironment for cancer research. Particularly, with serious concern, it is to be viewed that breast cancer is

✉ Selvaraj Kunjiappan
selvapharmabio@gmail.com

[1] Sir CV Raman-KS Krishnan International Research Center, Kalasalingam Academy of Research and Education, Krishnankoil 626126, India

[2] Department of Research and Development, Saraswathi Institute of Medical Sciences, NH-24, Anwarpur, Pilkhuwa, Hapur, Uttar Pradesh 245304, India

[3] School of Automotive and Mechanical Engineering, Kalasalingam Academy of Research and Education, Krishnankoil 626126, India

[4] School of Mechanical Engineering, Vellore Institute of Technology, Vellore 632014, India

[5] Department of Pharmaceutical Chemistry, MNR College of Pharmacy, Fasalwadi, Sangareddy, Telangana 502294, India

[6] Department of Pharmacy, Birla Institute of Technology and Science, Pilani 333031, India

[7] Department of Pharmaceutics, JSS College of Pharmacy, Rockland's, Ooty 643001, India

[8] Department of Pharmaceutical Biotechnology, JSS College of Pharmacy, Rockland's, Ooty 643001, India

reported to be the most common cause of cancer-related death among women globally (Ferlay et al. 2010). The American Cancer Society estimates that a total of 271,270 new breast cancer cases and 42,260 related cancer deaths are projected to occur in the United States in 2019 (Siegel et al. 2019). Last few decades have seen a major research endeavor towards adapting a combination of controlled drug release with less toxicity in anti-proliferative and apoptotic effectiveness in cell death.

Chemotherapy has often been the most chosen way of treating breast cancers, but it has many limitations. The major limitation is abnormal high mutability of many cancer cells escaping anticancer therapy (due to heterogeneous populations of cancer cells). This may make them difficult to target with a single type of treatment as well as generate resistance to cancer cells against the drug (Alberts et al. 2002). The cells can acquire drug resistance through various mechanisms that include inhibition of apoptosis, induction of stress response genes, less uptake of drug, increase of drug efflux transporter, etc. The primary one is mutation and natural selection (Damaraju et al. 2003). Initially, cancer cells are sensitive to therapies, but, later, these neoplasms acquire resistance and show unresponsiveness towards the same therapy (Viloria-Petit et al. 2001). It is well known that chemotherapeutic agents reach almost all cells in the body and they kill healthy cells as well as cancer cells (Danhier et al. 2010). The hydrogel is an alternative drug formulation due to its advantages such as multifunctionality, controlled release, selectivity, pH sensitivity, and less toxicity (Peppas et al. 2000; Bastiancich et al. 2019). The hydrogel could, therefore, be an efficient drug release vehicle towards anticancer efficacy and so in case of breast cancer.

Hydrogel was developed as a kind of soft materials with hydrophilic, 3D cross-linked polymeric networks which might be considered to act smartly when water or biological fluids come in contact with functional groups of hydrophilic nature attached to the polymeric backbone (Lutolf and Hubbell 2003). High water absorption efficiency, porosity, and soft consistency of hydrogels made it to imitate the biological tissue performance parameters with high biocompatibility as a carrier of drug reservoirs which could overcome the conventional therapy (Caló and Khutoryanskiy 2015; Yahia et al. 2015; Ryu et al. 2010; Ninan et al. 2016; Kevadiya et al. 2011). This activity diminishes the inflammatory reaction in the biological tissues. Furthermore, hydrogels can behave like living tissue than any other class of synthetic biomaterials (Sahoo et al. 2008). The above-mentioned properties of hydrogel are novel vectors for controlled drug delivery systems.

The controlled release system is essential to deliver a constant supply of the drug in the body at calculated time frame usually at zero-order rate by continuous release (Hickey et al. 2002). In this way, it reduces fluctuations of drug levels, thereby controls the adverse effect while improving the efficacy of the treatment (Hoffman 1998; Lordi 1986). The drug design delivery is effective when it satisfies the physiological prerequisites as it reaches its organ-specific micro environments. In drug release methodology, oral delivery is altogether agreeable in the realm of drug design especially in administration of drugs (Leslie 1954). The pH sensitivity assumes a noteworthy part in oral drug release, because pH variability exists in the body microenvironments of the organs. Therefore, hydrogels could react positively due to pH variation and enable controlled release accordingly (Lin and Metters 2006).

The degree of pH sensitivity, controlled drug release, and oral route of administration in hydrogel formulation is depending on the selection of polymeric materials and its formation of polymeric networks. In general, hydrogel can be prepared from either natural or synthetic polymers or combination of both (Memic et al. 2015). Hydrogels grafted with synthetic polymer possessing some good (super-absorbent and stable) and bad (not eco-friendly and produces undesirable toxicities) properties. Aside from synthetic polymers, natural polymers possess inherent properties, such as biocompatibility, non-toxic and excellent carriers of drugs, in addition that biodegradability (Nair and Laurencin 2007). These two characteristically opposite properties once balanced through optimization techniques could be exploited for efficient drug release. The correlative and/or complementary approach of treatments could, in fact, mimic microenvironments through hydrogels, specifically in chemotherapy and hyperthermia, chemotherapy and radiotherapy, and chemotherapy and gene therapy (Sakamoto et al. 2010). In our study, we have investigated the utilization of Zein, acrylic acid, and *N*, *N*-methylene bisacrylamide for preparation of hydrogels a novel drug delivery vehicle. Zein is a class of alcohol soluble prolamine protein present in the maize endosperm, and its characteristic are hydrophobicity with biocompatible, biodegradable, and non-toxic in nature (Labib 2018). Furthermore, the hydrophobic nature of Zein is a major advantage to the developing of hydrogel which, however, can be overwhelmed by hydrolysis treatments, and by joining hydrophilic groups onto the Zein protein backbone (Gil and Hudson 2004). Acrylic acid is a commercially available super-absorbent which is a typical pH and electrically sensitive synthetic polymer. It is used for the preparation of pH-sensitive hydrogel for controlled drug delivery system (Zohuriaan-Mehr and Kabiri 2008). Acrylic acid monomers easily co-polymerized with some other monomers such as zein by graft polymerization using *N*, *N*-methylene bisacrylamide as cross-linking agent. Moreover, combination of natural and synthetic polymers could significantly improve the physical, chemical, biological, and mechanical properties which results in appropriate delivery system for complex biological system.

5-Fluorouracil (5-Fu or 5-fluoro-2,4-pyrimidinedione) is an antitumor and antimetabolite of the pyrimidine analog (PS and Joshi 2013). Since a few decades, it is available in market and further found to possess wide activity against solid tumors of stomach, breast, gastrointestinal tract, pancreas, colon, ovary, liver, brain, etc. 5-Fu interferes with nucleoside metabolism and can be combined with RNA and DNA. 5-Fu is effective from initiate to cytotoxicity and cell death (Peters and Ackland 1996). The continuous administration of 5-Fu not only produces impact on reduced resistance to cell death, but also generates toxic ROS to cancer cells as well as healthy cells (Johnstone et al. 2002). Many research report suggested that natural antioxidant compounds reduced toxic ROS generation during the course of chemotherapy (Trachootham et al. 2009; Barrera 2012). Furthermore, concurrent release of dual-drug molecules with different molecular targets could be a considered as an effective approach in overcoming drug resistance and thereby lowers the tumor metastasis (Dai and Tan 2015).

The antioxidant compounds modulated the cytotoxic effect of anticancer drugs towards the drug-resistant mutants of cancer cells (Florea and Büsselberg 2011). Rutin (Ru or quercitin-3-rutinoside) is one of the phenolic compounds extensively found in many plants which contributes to the antibacterial properties of the plant (Djeridane et al. 2006; Selvaraj et al. 2013). Ru is strong antioxidant molecules possess advantages over other well-known flavonoids. It is also non-toxic and non-oxidizable molecule (Calabro et al. 2005). Conceptually, dual impact of anticancer drugs with natural compound becomes a very novel approach in the realm of drug design (Carmeliet and Jain 2000).

Parenteral administration of 5-Fu produces numerous adverse reactions such as diarrhea, nausea, vomiting, stomach pain, hematological disorder, cardiac, and dermatological toxic effects (Eng 2009; Bashir et al. 2017). However, impact of oral route combination with appropriate release formulations fully reduced the side effects of 5-Fu (Kumari et al. 2010). Many reports suggested that several polymer materials used for encapsulation could deliver 5-Fu in vitro safely (Arıca et al. 2002; Da Costa and Moraes 2003; Aydin and Pulat 2012; Rama et al. 2015). In the current study, we made an effort to formulate and design a pH-sensitive Zein-*co*-acrylic acid hydrogel using *N*, *N*-methylene bisacrylamide as cross-linking agent. Various weight ratios of Zein, acrylic acid, and *N*, *N*-methylene bisacrylamide are used to formulate hydrogel. Latter formulated hydrogels are evaluated for its intrinsic viscosity, dynamic swelling at pH 1.2, diffusion coefficient, sol–gel fraction, and porosity of hydrogel through response surface methodology modeling approach. The physico-chemical properties of optimized hydrogels were investigated by FTIR, XRD, SEM-EDAX, and DSC. Furthermore, the optimized hydrogels are selected for loading dual drugs (5-Fu and Ru), and evaluated its anticancer efficiency against breast cancer cell lines (MDA-MB-231 and MCF-7). Moreover, the in vitro drug release mechanism at pH 1.2 and pH 7.4 was also studied using drug release rate kinetic models.

Experimental section

Materials

The chemicals, acrylic acid, *N*, *N*-methylene bisacrylamide, ammonium persulphate, and phosphate-buffered saline (PBS) were obtained from Fisher Scientific, Mumbai, India. Zein, rutin, acridine orange, ethidium bromide, 3-(4,5-dimethyl-2-thiazolyl)-2,5-diphenyl-tetrazolium bromide (MTT), fetal bovine serum (FBS), streptomycin, penicillin, and dulbecco's modified eagle's medium (DMEM) were supplied by Himedia Laboratories Pvt. Ltd., Mumbai, India. Alkem Laboratories Ltd., Mumbai, India gifted 5-fluorouracil. The chemicals and solvents were of analytical category and supplied by Merck, Mumbai, India.

Cell culture

The breast cancer cell lines (MBA-MD-231 and MCF-7) were procured from National Center for Cell Science (NCCS), Pune, India. Both cell lines were maintained in DMEM medium supplemented with 10% heat inactivated fetal bovine serum (FBS) and a 1% mixture of penicillin/streptomycin and amphotericin B at 37 °C and 5% CO_2 in a humidified atmosphere in a CO_2 incubator.

Preparation of Zein-*co*-acrylic acid hydrogel

The formations of cross-linked hydrogel were shown in Scheme 1. Hydrogels are formulated from zein, and acrylic acid using *N*, *N*-methylene bisacrylamide as cross-linking agent by graft polymerization technique. In addition, ammonium persulphate was used as an initiator/catalyst. A specified quantity of acrylic acid (18–38 g) was added to the solution of sodium hydroxide in 70% aqueous ethanol to prepare acrylic acid solution. Later, cross-linker (*N*, *N*-methylene bisacrylamide; 0.03–0.5 g) was added to acrylic acid solution. Zein (0.1–0.5 g) was added to 70% aqueous ethanol and stirred for 5 min at 70 °C in a thermostat water bath. Ammonium persulphate (0.5 g) was added as initiator to the protein (zein) solution. After stirring for 5 min, the protein solution was mixed with the solution containing *N*, *N*-methylene bisacrylamide and acrylic acid solution. Then, the resultant solution was incubated for 4 h at 70 °C in a water bath followed by immersion in distilled water for a total of 36 h, with change of distilled water for every 12 h yielded the required hybrid hydrogels.

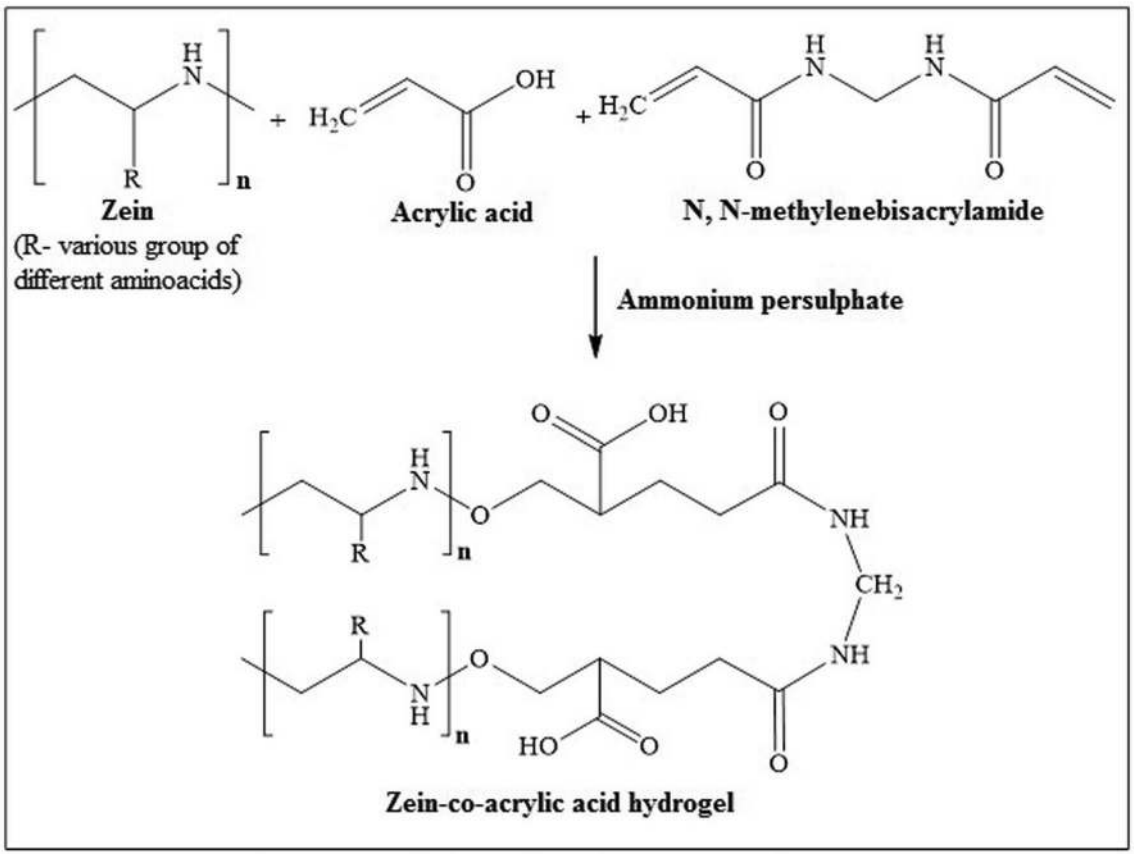

Scheme 1 Preparation of cross-linked Zein-*co*-acrylic acid hydrogel

Table 1 Experimental range of coded and actual values for central composite rotatable design (CCRD)

Independent variables (x_j)	Symbols	Factor levels		
		− 1	0	1
Zein (g)	X_1	0.3	0.1	0.5
Acrylic acid (g)	X_2	28	18	38
N,*N*-methylenebisacrylamide (g)	X_3	0.18	0.05	0.3

Experimental design

The best hydrogel combination was selected using optimization procedure adapting response surface methodology (RSM). For optimization of Zein-*co*-acrylic acid hydrogel, Zein (X_1: 0.1–0.5 g), acrylic acid (X_2: 18–38 g), and *N*, *N*-methylene bisacrylamide (X_3: 0.03–0.5 g) were suitably selected as the independent variables in RSM through central composite rotatable design (CCRD) as low, middle, and high values such as − 1, 0, and + 1; the number of experiments generated through RSM using Design Expert 11 software is depicted in Table 1. The formulations reside within the parameters with corresponding ranges are shown in Table 2. The intrinsic viscosity (y_1), dynamic swelling at pH 1.2 (y_2), diffusion coefficient (y_3), sol–gel fraction (y_4), and porosity (y_5) were taken as dependent variables. The interpreted parameters in matrix design corresponding to their responses are shown in Table 2. Correlation of dependent variable to independent variable was arrived using the second-order polynomial model by fitting experimental data. The model using response surface analysis is given in the following:

$$Y = \beta_0 + \sum_{i=1}^{3} \beta_i X_i + \sum_{i=1}^{3} \beta_{ii} X_i^2 + \sum_{i=1}^{2} \sum_{j=i+1}^{3} \beta_{ij} X_i X_j + \varepsilon. \quad (1)$$

In this study, Eq. (1) can be converted into the following equation according to the value of four variables:

$$Y = \beta_0 + \beta_1 X_1 + \beta_2 X_2 + \beta_3 X_3 + \beta_{11} X_1^2 + \beta_{22} X_2^2 + \beta_{33} X_3^2 + \beta_{12} X_1 X_2 + \beta_{13} X_1 X_3 + \beta_{23} X_2 X_3, \quad (2)$$

where Y is the dependent variables such as intrinsic viscosity (η), dynamic swelling (Q) at pH 4.2, diffusion coefficient (D), sol–gel fraction (%), and porosity (%); β_0 is the model

Table 2 Central composite rotatable design with experimental responses

S. no	Coded variable levels			Experimental value (Y)[a]					
	X_1	X_2	X_3	y_1	y_2	y_3	y_4		y_5
1	0.5	18	0.05	0.96	1.18	5.8	30.60	69.40	22.91
2	0.3	28	0.01	0.45	1.03	4.6	22.13	77.87	32.02
3	0.3	28	0.18	0.48	1.26	5.1	26.53	73.47	34.32
4	0.65	28	0.18	0.98	1.29	6.1	31.72	68.29	39.05
5	0.1	18	0.3	1.76	1.43	6.3	28.92	71.08	22.45
6	0.5	38	0.05	2.03	2.55	9.1	41.37	58.63	46.04
7	0.3	11.18	0.18	0.32	1.21	3.9	20.01	79.99	18.02
8	0.1	18	0.05	0.91	1.39	4.2	28.95	71.05	18.02
9	0.3	28	0.39	1.04	1.02	4.9	32.95	67.05	29.23
10	0.5	38	0.3	1.91	2.13	8.5	36.46	63.54	42.81
11	0.01	28	0.18	0.72	1.35	5.3	26.48	73.59	33.52
12	0.1	38	0.3	1.68	2.02	8.3	34.83	65.17	38.43
13	0.3	28	0.18	0.42	1.32	4.9	23.49	76.51	34.21
14	0.5	18	0.3	0.56	1.13	4.6	26.16	73.84	21.09
15	0.3	28	0.18	0.49	1.36	5.3	25.82	74.18	31.02
16	0.3	44.81	0.18	1.98	2.45	8.8	35.78	64.21	43.23
17	0.3	28	0.18	0.45	1.38	5.6	25.83	74.17	32.45
18	0.3	28	0.18	0.42	1.31	5.9	24.81	75.18	34.01
19	0.1	38	0.05	1.89	2.18	7.8	33.44	66.56	39.56
20	0.3	28	0.18	0.45	1.45	5.3	26.81	73.19	34.01

[a]All the experiments were repeated three times

constant; β_i, β_{ii}, and β_{ij} are model coefficients; X_i and X_j are coded value of independent variables; ε is error. Furthermore, the optimized hydrogel characteristic properties were examined using SEM, FTIR, DSC, and XRD to load dual drugs as well as to analyze release rate kinetics and anticancer activity.

Intrinsic viscosity (y_1)

The intrinsic viscosity of the hydrogel was performed in 0.5 N NaCl solution at 25 ± 0.1 °C in an automatic system Ubbelohde capillary-type viscometer which allows the reading of flow times of the sample taken automatically (Omer et al. 2016). Preparation of hydrogel solution involves mixing it with 0.5 N NaCl using magnetic stirrer for 24 h at ~ 25 °C. The molarity of NaCl in the hydrogel solution was maintained constant throughout the experiment. The result was derived with Huggins Eq. (3) using the criteria of dilute solution:

$$\eta_{sp}/c = [\eta] + bc, \tag{3}$$

where η is the intrinsic viscosity; η_{sp} is the specific viscosity; b is the Huggins parameter; c is the polymer concentration.

Dynamic swelling (y_2)

The pH-responsive dynamic swelling properties of the formulated hydrogels were determined by gravimetric method (Brazel and Peppas 1995). Small pieces (~ 5 mm-diameter disks) of dried hydrogels were precisely weighed and incubated in buffer solution of pH 1.2 at 37 ± 1 °C for 2 h. 0.2 M potassium chloride was used to adjust the ionic strength of buffer solution. The swollen disks removed at equilibrium from the solution were re-weighed after surplus surface water was completely dried out. Using the following Eq. (4), the swelling ratio (Q) was calculated by the following:

$$Q = \left(W_f - W_i\right)/W_i, \tag{4}$$

where W_f and W_i are the final and initial weights of the swollen disk, respectively. Experiments were performed in triplicate.

Diffusion coefficient (y_3)

Diffusion coefficient is one of the main criteria for drug release from cross-linked hydrogel (Langer and Peppas

1981). Following Eq. (5), is used to determine the water diffusion coefficient of hydrogel:

$$D = \pi\left(\frac{h\theta}{4Q_{eq}}\right)^2, \quad (5)$$

where, D is diffusion coefficient of the hydrogel; Q_{eq} is the swelling of the gel at equilibrium; θ is the slope of the linear part of the swelling curves; h is the initial sample thickness before swelling.

Sol–gel fraction (y_4)

Hydrogel samples were further freshly prepared into small disks with a diameter of ~ 5 mm, dried in a vacuum oven at 45 °C to achieve constant weight (W_o), and passed through Soxhlet extractor for 4 h with deionized water as solvent (Alla et al. 2007). Uncross-linked polymer identified in this extraction process was subsequently removed from the gel structure. Furthermore, through drying of the extracted gels in a vacuum oven at room temperature to constant weight (W_1), the sol–gel fraction was determined using Eqs. (6) and (7):

$$\text{Sol fraction } (\%) = \left[W_0 - W_1/W_1\right] \times 100 \quad (6)$$

$$\text{Gel fraction } (\%) = 100 - \text{Sol fraction.} \quad (7)$$

Porosity measurement (y_5)

Solvent replacement method (Yin et al. 2007) was followed to determine the porosity by immersing the dried hydrogel in ethanol overnight and weighed after excess ethanol on the surface was blotted. Thus porosity was determined using the following equation:

$$\text{Porosity} = \left(M_2 - M_1\right)/\rho V \times 100, \quad (8)$$

where M_1 and M_2 are the mass of hydrogel before and after immersion in ethanol respectively; ρ is the density of absolute ethanol; V is the volume of the hydrogel.

Preparation of 5-Fu and Ru-loaded hydrogel

Through optimization process, hydrogel with highest dynamic swelling at pH 1.2 was selected for further drug loading and releasing studies. 5-Fu- and Ru-loaded hydrogel was prepared using swelling equilibrium technique (Ranjha et al. 2010). The small pieces of hydrogel (~ 5 mm disks) were swelled using drug solution [1% w/v (5-Fu and Ru)] in ethanol–water mixture (50:50% w/v) at room temperature (28 ± 1 °C) for 3 day incubation, to ensure that the drug in the solution was adsorbed onto the hydrogel. After the process of drug adsorption in the swelled hydrogel, the hydrogel was further washed with distilled water to remove the adhered drugs on the surface. The hydrogel obtained above was initially dried at room temperature and dried in oven at 40–45 °C for 1 week to completely remove the absorbed solvent.

Determination of the entrapped 5-Fu and Ru

The hydrogel samples placed in a 30 ml phosphate-buffered solution (pH 7.5) were stirred for 48 h to determine the drug loading and encapsulation. The filtered solution was assayed by UV–visible spectrophotometric method at 266 nm for 5-Fu and 300 nm for Ru, respectively. Using Eqs. (9) and (10), the percent of drug loading and encapsulation efficiency were determined:

$$\text{Drug loading } (\%) = \text{Weight of drug in gel/Weight of gel} \times 100 \quad (9)$$

$$\text{Encapsulation efficiency } (\%) = \text{Total weight of drug} - \text{Free drug/Total drug} \times 100 \quad (10)$$

Physico-chemical characterization

Fourier transform infrared spectroscopy (FTIR)

The chemical bonding and interactions between Zein protein, and acrylic polymer and drugs in the optimized hydrogel were determined by Fourier transform infrared spectroscopy (Shimadzu IR Tracer-100) using potassium bromide (KBr). Briefly, a small amount of Zein, 5-Fu, Ru, finely grounded powder hydrogel (unloaded) and 5-Fu- and Ru-loaded hydrogel were mixed with IR grade KBr (1:50) to prepare a round disk using a small hydraulic press. Later, the FTIR characteristic spectrum of above prepared round disk was recorded in the frequency of 500–4000 cm^{-1} with resolution of 4 cm^{-1}.

Scanning electron microscopy (SEM)–energy-dispersive X-ray spectroscopy (EDX)

The SEM analysis was used to evaluate the surface topography and morphological arrangements of the optimized cross-linked hydrogel and dual drug-loaded hydrogel. Both the hydrogel, i.e., unloaded and drug-loaded hydrogel, were air dried and mounted on SEM sample stubs for subsequent morphological arrangements study under a Carl Zeiss EVO 18 scanning electron microscope at 20 kV. An EDX detector (Bruker XFlash 5010 123 eV) was used for elemental analysis of mineral grown on hydrogels.

X-ray diffraction (XRD)

The physical nature of cross-linked hydrogel (unloaded) and dual drug-loaded hydrogel were observed in an X-ray

diffractometer using a copper radiation source. Prior to that, hydrogel (unloaded) and dual drug-loaded hydrogel were grounded to a fine powder. The XRD scanning at a voltage of 20 keV and a current of 30 mA with Cu Kα 1 radiation ($l = 0.1542$) in a two-theta (degree) configuration was carried out using A BRUKER D 8 Advance ECO XRD system with SSD160 1 D Detector.

Differential scanning calorimetry (DSC)

DSC analysis was carried out to assess the crystal or melting characteristics of the cross-linked hydrogel (unloaded) and with drugs loaded hydrogel. DSC was recorded with NETZSCH differential scanning calorimeter (DSC 204) at 10 °C min^{-1} heating rate under a stream of nitrogen (20 mL min^{-1}). Accurately weighed 3 mg of samples were placed in an aluminum pan in a hermetically sealed condition. Measurements were performed in nitrogen atmosphere at 40–500 °C temperature.

In vitro drug release studies

USP-dissolution apparatus-II (Labline, India) was used to study the in vitro drug release at 37 ± 0.5 °C. Dual drug-loaded hydrogel disk was placed in 200 mL phosphate-buffered saline (pH 1.2 and 7.4) and drug release was observed continuously for 6 h at 100 rpm paddle speed. About 5 mL of sample was withdrawn at determined time points, and replaced with an equal volume of fresh medium. Methanol was used to dissolve the collected resultant supernatant. Furthermore, the solution was centrifuged in 14,000×*g* at 25 °C. The resulting solution was used for UV–visible spectrophotometric analysis at 266 nm for 5-Fu and 300 nm for Ru. Drug release experiments were followed in triplicate and obtained the average value using the following equation:

$$\% \text{ DRC} = \text{Released drug from hydrogel} / \text{Total drug in the hydrogel} \times 100. \quad (11)$$

Analysis of drug release kinetics

The in vitro drug release mechanism was studied using zero-order, first-order, Higuchi, Korsmeyer–Peppas, and Hixson–Crowell models. DD Solver 1.0 software was used to get analytical data to understand the kinetic release model (Ranjha and Qureshi 2014). The estimation of n exponent in Korsmeyer–Peppas demonstrates whether the order of release is Fickian or non-Fickian. If, $n = 0.45$, order of release is Fickian, whereas $n = 0.89$ corresponds to case II transport, while $0.45 < n > 1.0$, the diffusional mechanism is non-Fickian. No kinetic data or n values were calculated when swelling and drug release was not significant.

Anticancer effect of released 5-Fu and Ru

The in vitro cytotoxicity of hydrogel released 5-Fu and Ru was screened by MTT assay method (Kunjiappan et al. 2018) on breast cancer cell lines (MBA-MD-231 and MCF-7). In brief, cancer cells were seeded in 96-multiwell plate (Tarsons India Pvt. Ltd., Kolkata, West Bengal, India) with 1×10^5 cells per well in 100 µL of DMEM at 37 °C in a 5% CO_2 atmosphere for 24 h. After pre-determined time of incubation, culture medium was replaced with fresh DMEM medium with various concentrations (5–150 µg mL^{-1} 5-Fu and Ru-loaded hydrogel, and 100 µg mL^{-1} of 5-Fu and 100 µg mL^{-1} of Ru) for 24 h incubation. The respective amount of DMSO in phosphate-buffered saline was used instead of hydrogel as control. The medium was removed after 24 h to wash the cells with phosphate-buffered saline (PBS, 0.01 M, pH 7.4). Later, 200 µL (5 mg mL^{-1}) of 0.5% 3-(4, 5-dimethyl-2-thiazolyl)-2, 5-diphenyl-tetrazolium bromide (MTT) prepared in serum-free medium solution was added to each well and incubated for 4 h at 37 °C in a 5% CO_2. Thereby obtained cells were fixed, washed, and stained with MTT. Excess stain and attached cells were removed using acetic acid and Tris-EDTA buffer, respectively. The color intensity was measured in a Spectramax M2 Microplate Reader (Molecular Diagnostic, Inc.) at a wavelength of 550 nm. The ratio of the absorption of treated cells to absorption of non-treated cells expressed in percentage denotes percentage of death cells. Every treatment condition was repeated in triplicate and IC_{50} of 5-Fu and Ru-loaded hydrogel was subsequently used for further studies.

Measurement of apoptosis by acridine orange/ethidium bromide (AO/EB) double staining

Apoptosis of the cancer cells were investigated by fluorescence microscopy after staining with AO/EB (Ramalingam et al. 2016). Briefly, MDA-MB-231 cancer cells were seeded on a cover slip in a 24-well plate (1×10^5 cells/well) with addition of appropriate amount of 5-Fu and Ru-loaded hydrogel IC_{50} was incubated. After being cultured for 72 h, 20 µL of trypsin was added to each well. Cover slip was removed from 24-well plate and washed with 1 × PBS buffer. Later, it was treated with dual fluorescent stain 10 µL mL^{-1} containing acridine orange (10 mg mL^{-1}) and ethidium bromide (10 mg mL^{-1}) and incubated again for another 30 min. After incubation, unbound dyes were washed with 1 × PBS buffer. The morphology of apoptotic cells was examined under fluorescence microscope and representative fields were captured at 40 × magnification. Dual AO/EB staining method was repeated for three times.

Determination of intracellular ROS (reactive oxygen species) levels

The intracellular generation ROS of control and 5-Fu and Ru-loaded hydrogel-treated cells were quantified using DCFH-DA fluorescence dye which can pierced into the cells (intracellular matrix) where ROS oxidizes it to fluorescent dichlorofluorescence (DCF) (Kunjiappan et al. 2018). In 6-well culture plate for 24 h period, cells (MCF-7; 1×10^5 cells well^{-1}) are seeded and incubated. After the incubation period of 24 h, cells are treated with 10% FBS supplemented IC_{50} concentration of 5-Fu and Ru-loaded hydrogel for 24 and 48 h further incubation. Thereafter, 1 × PBS was used to wash the cells twice; at 37 °C for 15 min, it is labeled with DCFH-DA (20 µM) and kept on ice, filtered using Cell Strainer (70 µM). Afterwards, H_2O_2 (100 µM) replaces DCFH-DA into the cells and additionally incubated for 45 min. At 475 nm λ_{ex} and 525 nm λ_{em} using fluorescence spectrophotometer monitored the change in the fluorescence.

Statistical analysis

The Design expert software (Stat-Ease Inc., USA 11.0) was used to develop hydrogel formulations and optimization studies. The data are presented as the mean ± standard deviation (SD), and experiments for each sample were performed three times. Each experimental result was statistically analyzed through the one-way analysis of variance (ANOVA) and Dunnett's multiple comparison tests. A value of $P < 0.05$ was considered statistically significant, and $P < 0.01$ was considered highly significant. Statistical analyses and graphing were performed using SPSS statistics version 20.0 software (SPSS Inc., Chicago, IL, USA).

Results

Optimization

The RSM was successfully applied for the preparation of cross-linked and pH-sensitive hydrogel for oral administration of cancer therapeutics in oral treatment of breast cancer. In optimization, a total of 20 formulations were generated through RSM. Each formulation is optimized based on the coded level of low (− 1), middle (0), and high (+ 1) values of independent variables such as Zein, acrylic acid, and *N*, *N*-methylene bisacrylamide. For optimization five dependent parameters, namely, intrinsic viscosity, dynamic swelling at pH 1.2, diffusion coefficient, sol–gel fraction, and porosity of hydrogel, were also taken. The independent variables are investigated against dependent parameters, and observed experimental values are listed in Table 2. Optimization was performed on the basis of individual experimental results and their statistical analyses. From the RSM, the cross-linked and pH-sensitive hydrogel was obtained at a combination of 0.5 g Zein, 38 g acrylic acid, and cross-linker 0.05 g of *N*, *N*-methylene bisacrylamide. At this combination, the prepared hydrogel has 2.03 viscosity (η), 2.55 dynamic swelling (Q) at pH 1.2, 9.1 diffusion coefficient (D), 41.36-58.63% sol–gel ratio, and 46.04% porosity. The experimental results were used to analyze the coefficients of the second-order polynomial equation and Table 3 shows the results of fitting quadratic models with the data. The significance of the coefficients was analyzed by performing the analysis of variance statistical tool. The fitness of the model was verified through lack of fit test ($P < 0.0001$), which indicated the suitability of the models. The F test was performed to verify the significance of each coefficient. It could be learned that if F value becomes greater and P value becomes smaller, then the corresponding variables are said to be more significant (Selvaraj et al. 2014). The found F value (8.05) and P value (0.0500) clearly indicate that the model was highly significant. Furthermore, the second-order polynomial equation for the fitted quadratic model for dependent coded variables is given in the following equations:

$$y_1 = 0.3986 - 0.0595X_1 + 0.4475X_2 + 0.0361X_3 + 0.2935X_1^2 + 0.3421X_2^2 + 0.275X_3^2 - 0.19X_1X_2 - 0.145X_1X_3 - 0.0975X_2X_3 \quad (12)$$

$$y_2 = 1.31 - 0.0208X_1 + 0.4273X_2 - 0.0533X_3 + 0.0861X_1^2 + 0.0248X_2^2 - 0.0155X_3^2 + 0.1237X_1X_2 - 0.0438X_1X_3 - 0.0713X_2X_3 \quad (13)$$

$$y_3 = 5.24 + 0.1531X_1 + 1.54X_2 + 0.0652X_3 + 0.4567X_1^2 + 0.6034X_2^2 + 0.1031X_3^2 + 0.2X_1X_2 - 0.55X_1X_3 - 0.1250X_2X_3 \quad (14)$$

$$y_4 = 24.94 + 1.04X_1 + 4.25X_2 + 0.2601X_3 + 2.42X_1^2 + 1.64X_2^2 + 2.41X_3^2 + 1.33X_1X_2 - 1.34X_1X_3 + 0.1187X_2X_3 \quad (15)$$

$$y_5 = -5.9666 - 9.9008X_1 + 1.5379X_2 + 62.52139X_3 + 21.6260X_1^2 - 0.0114X_2^2 - 93.2281X_3^2 + 0.45813X_1X_2 - 41.75X_1X_3 - 0.697X_2X_3, \quad (16)$$

Analysis of the model

To analyze the interactive effect of the independent parameters (X_1, X_2, and X_3) on the 3D response surface plot, contour

Table 3 Analysis of variance (ANOVA) for the quadratic polynomial mode

Source	Sum of square	*df*	Mean square	*F* value[a]	*P* value[b]
Intrinsic viscosity (η) (y_1)[c]					
Model	6.6238	9	0.7359	8.0523	0.0015
X_1	0.0450	1	0.0450	0.4931	0.4986
X_2	2.7351	1	2.7351	29.925	0.0002
X_3	0.0158	1	0.0158	0.1731	0.6860
X_1X_2	0.2888	1	0.2888	3.1597	0.1058
X_1X_3	0.1682	1	0.1682	1.8402	0.2047
X_2X_3	0.0760	1	0.0760	0.8320	0.3831
X_1^2	1.0183	1	1.0183	11.141	0.0075
X_2^2	1.7071	1	1.7071	18.677	0.0015
X_3^2	0.8123	1	0.8123	8.8877	0.0137
Residual	0.9140	10	0.0914		
Lack of fit	0.9097	5	0.1819	212.387	< 0.0001
Pure error	0.0043	5	0.0008		
Cor total	7.5379	19			
Dynamic swelling at pH 1.2 (y_2)[d]					
Model	3.6772	9	0.4085	8.7159	0.0011
X_1	0.0055	1	0.0054	0.1170	0.7393
X_2	2.4934	1	2.4934	53.1914	< 0.0001
X_3	0.0344	1	0.0343	0.7332	0.4118
X_1X_2	0.1225	1	0.1225	2.6135	0.1370
X_1X_3	0.0153	1	0.0153	0.3266	0.5802
X_2X_3	0.0406	1	0.0406	0.8663	0.3738
X_1^2	0.0877	1	0.0877	1.8715	0.2012
X_2^2	0.8886	1	0.8886	18.9568	0.0014
X_3^2	0.0025	1	0.0025	0.0547	0.8197
Residual	0.4687	10	0.0468		
Lack of fit	0.4472	5	0.0894	20.7691	0.0023
Pure error	0.0215	5	0.0043		
Cor total	4.1459	19			
Diffusion coefficient (y_3)[e]					
Model	43.253	9	4.8059	8.6561	0.0011
X_1	0.2981	1	0.2981	0.5369	0.4805
X_2	32.417	1	32.417	58.3875	< 0.0001
X_3	0.0514	1	0.0514	0.0927	0.7669
X_1X_2	0.32	1	0.32	0.5763	0.4652
X_1X_3	2.42	1	2.42	4.3587	0.0633
X_2X_3	0.125	1	0.125	0.2251	0.6453
X_1^2	2.4655	1	2.4655	4.4408	0.0613
X_2^2	5.3098	1	5.3098	9.5636	0.0113
X_3^2	0.1139	1	0.1139	0.2053	0.6601
Residual	5.5520	10	0.5552		
Lack of fit	4.9170	5	0.9834	7.7434	0.0211
Pure error	0.635	5	0.127		
Cor total	48.8055	19			
Sol–gel fraction (%) (y_4)[f]					
Model	460.5831	9	51.1751	5.4431	0.0070
X_1	13.7951	1	13.7951	1.4672	0.2536
X_2	246.2745	1	246.274	26.1939	0.0004
X_3	0.8196	1	0.8196	0.0871	0.7738
X_1X_2	14.2471	1	14.2471	1.5153	0.2464
X_1X_3	14.3514	1	14.3514	1.5264	0.2448
X_2X_3	0.1127	1	0.1127	0.0119	0.9149
X_1^2	69.3082	1	69.3082	7.3716	0.0217
X_2^2	39.0524	1	39.0524	4.1536	0.0688
X_3^2	62.0986	1	62.0986	6.6048	0.0278
Residual	94.0196	10	9.40196		
Lack of fit	86.5166	5	17.3033	11.5308	0.0089
Pure error	7.5030	5	1.5006		
Cor total	554.6028	19			
Porosity (%) (y_5)[g]					
Model	1260.010	9	140.0011	35.4737	< 0.0001
X_1	37.6105	1	37.6105	9.5298	0.0115
X_2	1139.8710	1	1139.871	288.8229	< 0.0001
X_3	0.8744	1	0.8744	0.2215	0.6479
X_1X_2	6.7161	1	6.7161	1.7017	0.2212
X_1X_3	8.7153	1	8.7153	2.2083	0.1681
X_2X_3	6.0726	1	6.0726	1.5386	0.2431
X_1^2	8.8460	1	8.8460	2.2414	0.1652
X_2^2	19.0358	1	19.0358	4.8233	0.0527
X_3^2	22.7400	1	22.7400	5.7619	0.0372
Residual	39.4660	10	3.94660		
Lack of fit	30.6765	5	6.1353	3.4901	0.0981
Pure error	8.7895	5	1.7579		
Cor total	1299.476	19			

df Degrees of freedom

[a]Test for comparing model variance with residual (error) variance

[b]Probability of seeing the observed *F* value if the null hypothesis is true

[c]Std dev: 0.3023; mean: 0.9950

[d]Std dev: 0.2165; mean: 1.52

[e]Std dev: 0.7451; mean: 6.01

[f]Std dev: 3.07; mean: 29.15

[g]Std Dev: 1.99; Mean: 32.32

plot and second-order polynomial equation are used. From Eqs. (12) to (16) and experimental values in Table 3, it was found that the properties of viscosity, dynamic swelling at pH 1.2, diffusion coefficient, sol–gel fraction, and porosity of formulated hydrogel not only involved, but the linear term of X_1, X_2, and X_3 and quadratic term X_1^2, and interaction term of X_1X_2, X_2X_3 are also contributed. The pH-sensitive property of formulated hydrogel was clearly explained through 3D response surface plot and contour plot (Fig. 1). The observed correlation coefficient (r^2) value (0.08787) and *P*

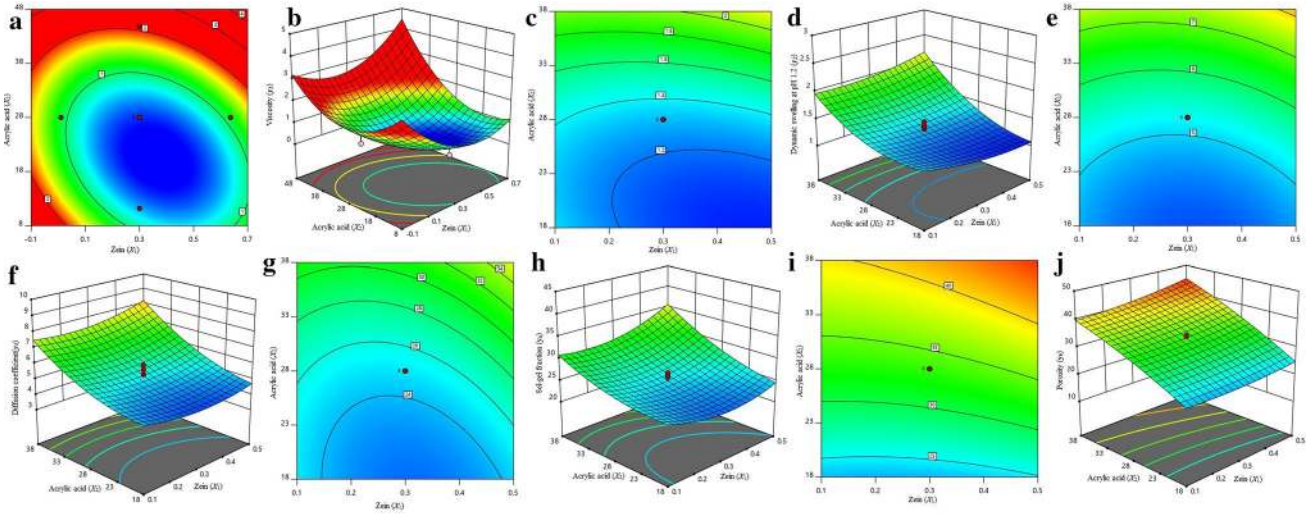

Fig. 1 Response surface and contour plots showing the combined effects of Zein (X_1) and Acrylic acid (X_2) for maximum intrinsic viscosity (η) (**a**, **b**), dynamic swelling at pH 1.2 (**c**, **d**), diffusion coefficient (**e**, **f**), sol–gel fraction (**g**, **h**), and porosity (**i**, **j**), when concentration of *N*, *N*-methylene bisacrylamide (X_3) was held at fixed level (zero level = 0.05 g)

value of lack-of-fit ($P < 0.0001$) proves that the model was significant.

Hydrogel preparation and drug loading and encapsulation efficiency

The cross-linked and pH-sensitive Zein-*co*-acrylic acid hydrogel was successfully prepared by graft polymerization technique. Furthermore, 5-Fu and Ru-loaded hydrogel was also prepared by swelling equilibrium method. Figure 2 shows the diagram of the unloaded hydrogel dry powder (a), dual drug-loaded hydrogel dry powder (b), water-swollen unloaded hydrogel (c), and water-swollen dual drug-loaded hydrogel (d). The observed drug loading efficiency of 5-Fu and Ru was found to be 12.13% and 10.86%, respectively, and encapsulation efficiency of 5-Fu and Ru was 89.35% and 81.47%, respectively.

Physico-chemical characterization

FTIR

FTIR spectra of Zein, Ru, 5-Fu, Zein-*co*-acrylic acid hydrogel, and 5-Fu and Ru-loaded Zein-*co*-acrylic acid hydrogel are depicted in Fig. 3. The characteristic peaks of Zein was observed at 3440 cm^{-1} (O–H stretching), 2880 cm^{-1} (C–H stretching of vibration), 1640 cm^{-1} (C=O group), 1556 cm^{-1} (amide group), and 1098 cm^{-1} (C–N stretching). The hydrogel spectrum shows peaks at 1680 cm^{-1} (COO group) and peak at 1490 cm^{-1} indicates the formation of complexation (hydrogel) with amino group of Zein and carboxylic group of acrylic acid. The spectra of 5-Fu and Ru have confirmed

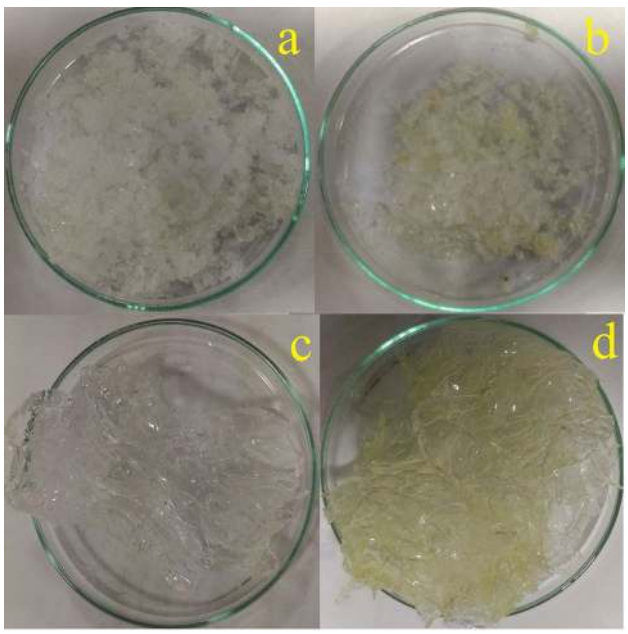

Fig. 2 Hydrogel (unloaded) dry powder (**a**), 5-Fu and Ru-loaded hydrogel dry powder (**b**), water-swollen unloaded hydrogel (**c**), and water-swollen 5-Fu and Ru-loaded hydrogel (**d**)

that both drug-loaded hydrogels have all characteristic peaks as mentioned in the peaks of 5-Fu and Ru. In addition, there is no significant shift in major peaks, which demonstrates that there is no chemical interaction between the polymer and the drugs used.

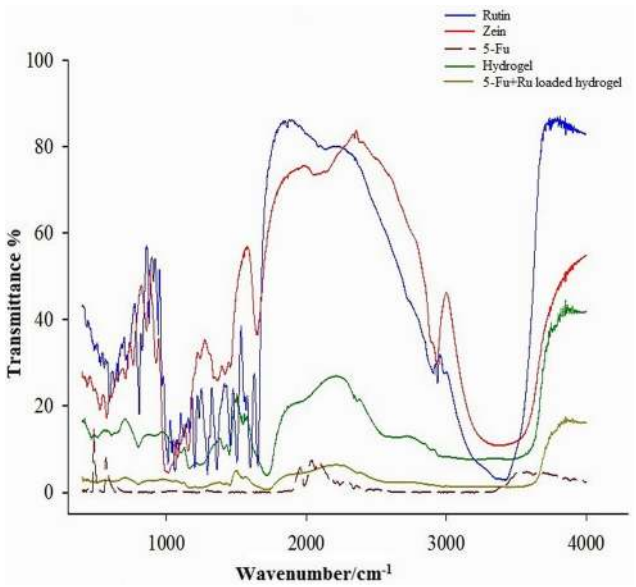

Fig. 3 FTIR spectrum of Ru, Zein, 5-Fu, hydrogel (unloaded), and 5-Fu and Ru-loaded hydrogel

SEM–EDX

Studies of SEM were performed to characterize the microstructure and surface topography of the prepared Zein-*co*-acrylic acid hydrogel and drug-loaded hydrogel. Figure 4a–c shows the images of unloaded freeze dried hydrogel with various magnifications. First image (Fig. 4a) clearly shows the well-defined macro pore structure on the surface of unloaded hydrogel, with pores diameter in the range of 18–20 µm. Furthermore, Fig. 4b, c shows the interconnection between pores and that could be assigned by formation of cross-linking network with *N*, *N*-methylene bisacrylamide. The interconnection could be attributed to the organization of amide groups of Zein and carboxylic groups of acrylic acid. In contrast, Fig. 4d–f observes that surface morphology of 5-Fu and Ru-loaded hydrogel was changed. The drug-loaded hydrogel smoothly interconnected with pores and no connection or interaction between the loaded drugs.

The EDX analyses of pure hydrogel and 5-Fu and Ru-loaded hydrogel are depicted in Fig. 5a, b, respectively. In both images, the strong signals for elemental ions of C, O, Mg, K. Al, Si, Na, and Ca are observed. The increased level of oxygen in the drug-loaded hydrogel indicates that drugs (OH) are linked on the hydrogel.

X-ray diffraction

Figure 6 displays the X-ray diffraction pattern of unloaded hydrogel and 5-Fu and Ru-loaded hydrogel. The X-ray diffractogram of hydrogel showed two broad peaks at 2θ equaled to 4° and 16° due to the amorphous nature. The observed low-intensity peaks illustrated that Zein cross-linked with acrylic acid polymer.

DSC

DSC measurements were carried out to evaluate the changes in the thermal behavior of the Zein-*co*-acrylic acid hydrogel

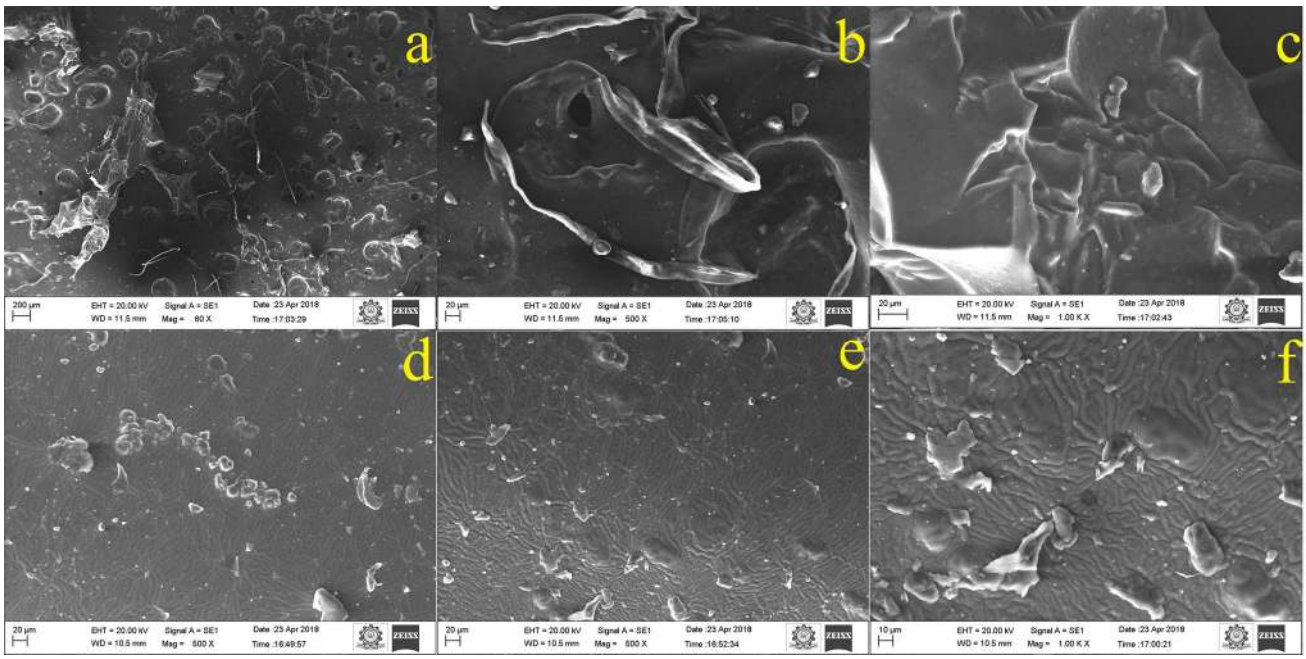

Fig. 4 Microstructure and surface topography of hydrogel (unloaded) (**a**–**c**) and 5-Fu and Ru-loaded hydrogel (**d**–**f**)

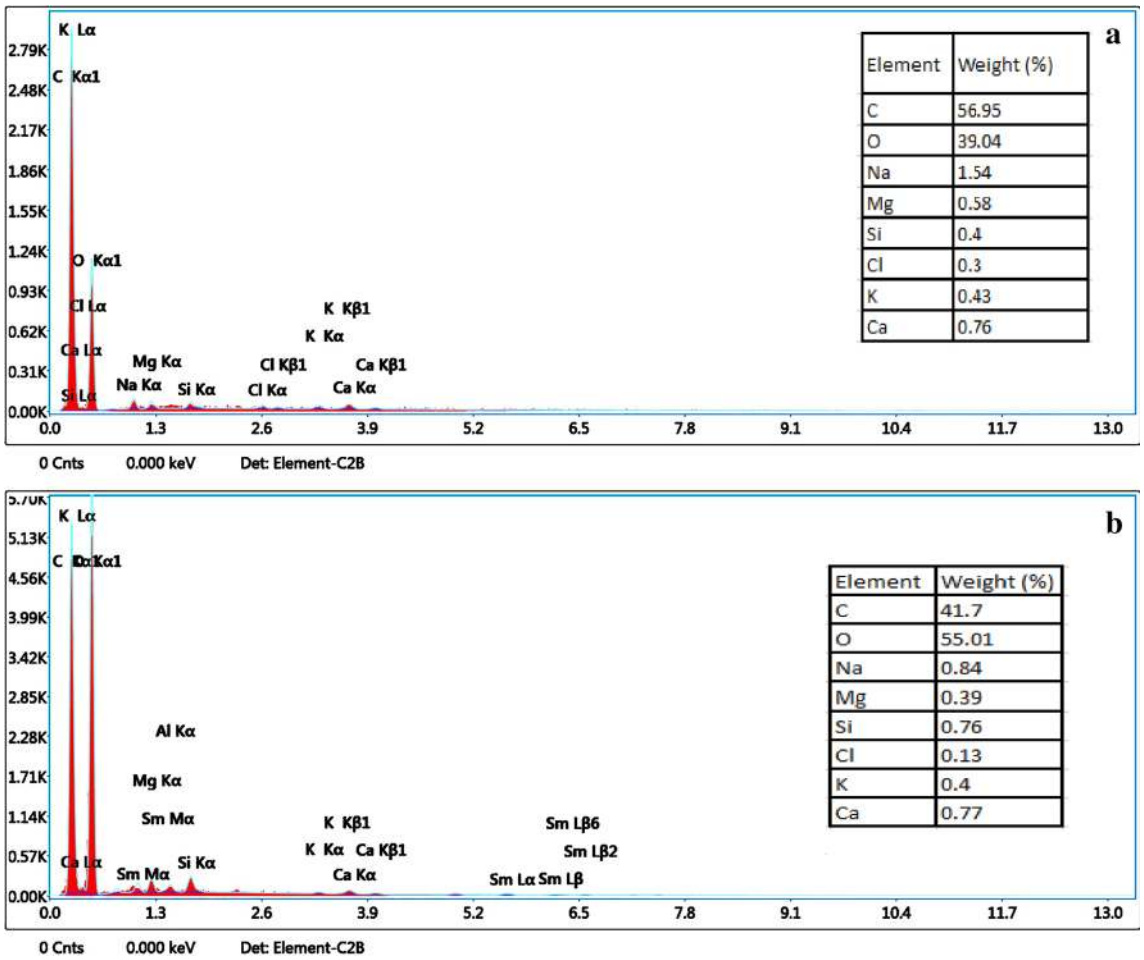

Fig. 5 Elements of hydrogel (unloaded) (**a**) and 5-Fu and Ru-loaded hydrogel (**b**)

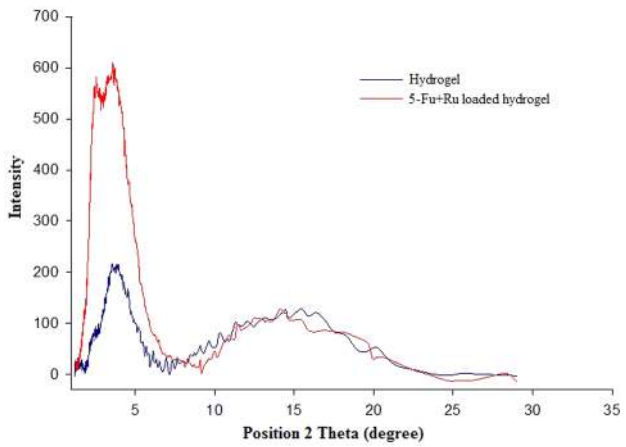

Fig. 6 XRD spectra of hydrogel (unloaded) and 5-Fu and Ru-loaded hydrogel

and drug-loaded hydrogel. DSC thermocurve depicted in Fig. 7 shows initial endothermic peak at 145 °C (pure hydrogel) and 150 °C (drug-loaded hydrogel) due to removal of absorbed moisture. From the curves, we observed that there is no glass-to-liquid transition-onset peak. The drug-loaded hydrogel showed that endothermic peak at 240 °C represents decompositions of loaded drugs and sharp second peak at 261.8 °C indicates the decomposition of hydrogel.

Drug release studies

In vitro release of 5-Fu and Ru from Zein-*co*-acrylic acid hydrogel was performed in USP-dissolution II apparatus using phosphate-buffered saline of pH 1.2 and 7.4 at 37 ± 0.5 °C. The obtained results are shown in Fig. 8. The accumulative release of 5-Fu and Ru from hydrogel was found to be 18.23% and 15.7% (pH 7.4); 17.5%, and 12.54% (pH 1.2) within 30 min, respectively. The highest amount of 5-Fu and Ru released from hydrogel were 88.73% and

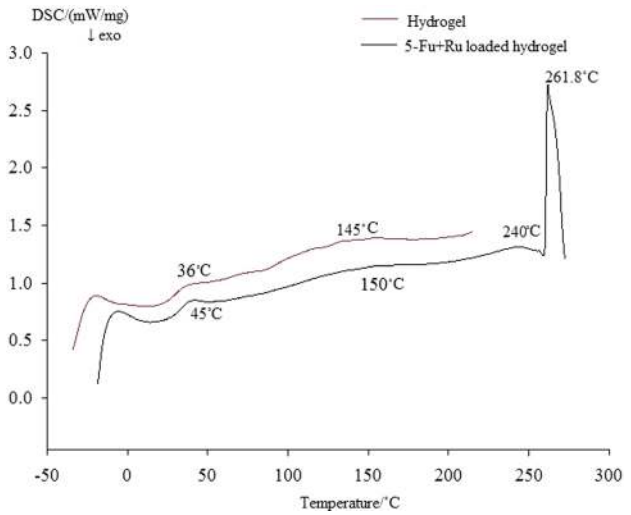

Fig. 7 Thermograph of hydrogel (unloaded) and 5-Fu and Ru-loaded hydrogel

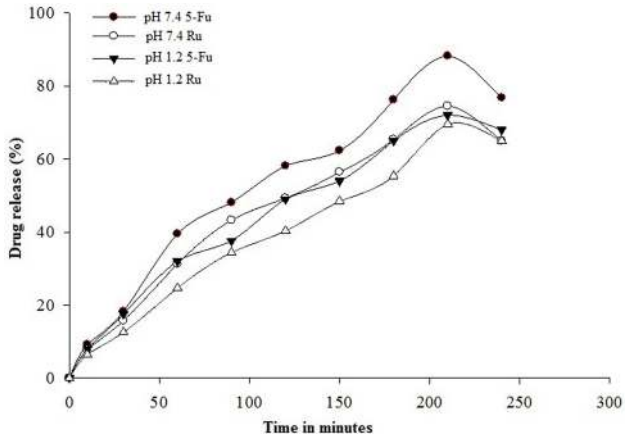

Fig. 8 In vitro 5-Fu and Ru-release pattern of 5-Fu and Ru-loaded hydrogel in pH 1.2 and pH 7.4 at 37 ± 0.5 °C in PBS buffer as a function of time. Data were represented as mean ± standard deviation ($n = 3$)

74.54% (pH 7.4); 72% and 69.54% (pH 1.2) within 210 min, respectively.

Drug release kinetics

Drug release data of the hydrogel were fitted into various kinetic models such as zero-order, first-order, Higuchi, Korsmeyer–Peppas, and Hixon–Crowell models. The drug release kinetics profile of various kinetic models is presented in Table 3. The correlation coefficient (r^2) values were calculated for each kinetic model and release rate constant is also predicted for these models. If the r^2 value is very close to 1, then it is considered to be best fit model. The r^2 values of first-order kinetics were observed higher than that of zero-order kinetics, i.e., 0.8340–0.9695 (5-Fu in pH 7.4), 0.8303–0.9680 (Ru in pH 7.4), 0.8703–0.9807 (5-Fu in pH 1.2), and 0.9441–0.9818 (Ru in pH 1.2) which is best fit for the models. Further, the values of r^2 in Higuchi model were in the range of 0.9695 (5-Fu in pH 7.4), 0.9680 (Ru in pH 7.4), 0.9807 (5-Fu in pH 1.2), 0.9818 (Ru in pH 1.2) that suggested the controlled drug release; while in Korsmeyer–Peppas model, the value of diffusion exponent (n) ranged from 0.62 to 0.75 with correlation coefficient (r^2) of 0.9585 to 0.9818. The resultant values indicated the non-Fickian behavior of hydrogel formulation. Furthermore, the diffusion exponent observed to be higher than 0.75 which implies that the drug release from the system follows Super case II transport. The higher r^2 values in Hixon Crowell model indicates uniform dissolution and constant amount of drug release from the hydrogel formulation. Overall drug release mechanism is predominantly controlled at a fixed quantity of drug release from the hydrogel formulation.

Cytotoxicity

Cytotoxicity studies of various concentrations of 5-Fu and Ru-loaded hydrogel using MTT assay on MDA-MB-231 and MCF-7 cancer cell lines. The 5-Fu and Ru-loaded hydrogel showed quantifiable cytotoxicity of cells in a dose-dependent manner, as shown in Fig. 9a. The dual drug of 5-Fu and Ru-loaded hydrogel with 52.5 µg mL^{-1} concentration has impacted that about 50% cell death at IC_{50} of 5-Fu and Ru-loaded was used for further study. The morphological changes in MCF-7 cells could also be observed using this formulation after being treated with a 60 µg mL^{-1} concentration of 5-Fu and Ru-loaded hydrogel, as shown in Fig. 10a, b.

Apoptosis analyses

The morphological changes due to induction of apoptosis by 5-Fu and Ru-loaded hydrogel in MDA-MB-231 cancer cell line were analyzed by AO/EB double staining method. After 48 h of treatment with 52.5 µg mL^{-1} concentration (IC_{50} value) of 5-Fu and Ru-loaded hydrogel, the cells were harvested and stained with AO/EB and viewed under fluorescence microscope. No significant apoptosis was observed in the negative control cells (Fig. 11a). In contrast, the 5-Fu and Ru-loaded hydrogel-treated cells showed round, irregular shape with condensed nuclei, distorted membrane, and apoptotic bodies (Fig. 11b).

ROS generation by 5-Fu and Ru-loaded hydrogel

The generation of ROS is one of the events that take place at the beginning of apoptosis. As shows in Fig. 12, the treatment of MCF-7 cancer cells with 5-Fu and Ru-loaded

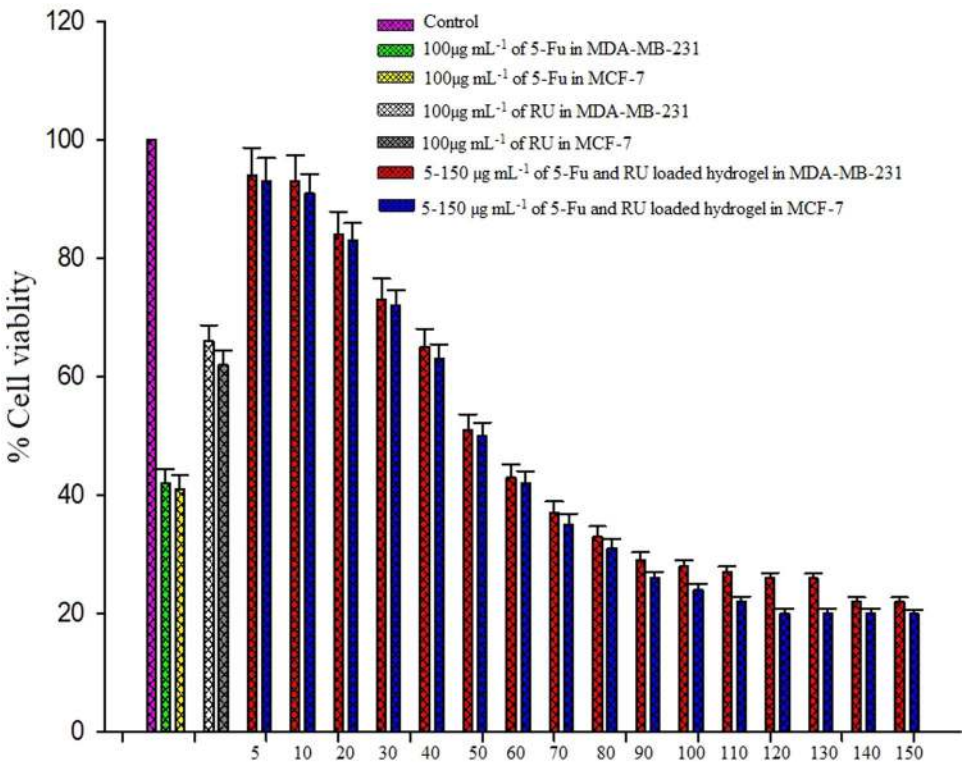

Fig. 9 In vitro cytotoxic screening of breast cancer (MDA-MB-231 and MCF-7) cells using different concentrations of 5-Fu and Ru-loaded hydrogels after 24 h treatment. The percentage of apoptotic cells increased dose dependently. Values are mean ± standard deviation of triplicate measurements ($P < 0.05$)

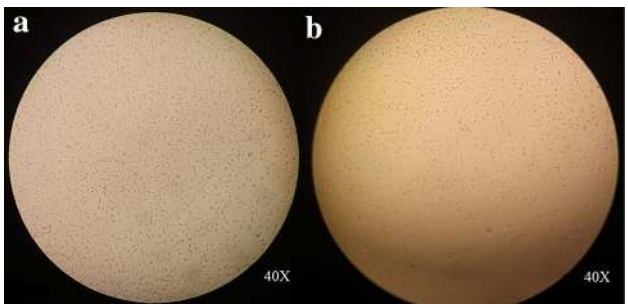

Fig. 10 Phase-contrast microscope images of MCF-7 cells showing the morphology of an un-treated cells (**a**) and treated cells with 5-Fu and Ru-loaded hydrogels (**b**)

hydrogel at concentration of 52.5 µg mL^{-1} significantly increased level of ROS as compared to control. It appeared that 5-Fu and Ru mainly induced the increased level of ROS production and its causing oxidative stress.

Discussion

Based on combination of natural and synthetic polymer, the pH-sensitive hydrogels showed their importance for oral administration of cancer therapeutics, with safe and controlled delivery for various solid tumors (Schmaljohann 2006). It is biocompatible, non-immunogenic, and biodegradable nature. Many researchers have been used drug-loaded hydrogels for the treatment of glioblastoma (Bastiancich et al. 2019). The natural polymers especially, protein or polysaccharides, are non-toxic and biodegradable (Malafaya et al. 2007). Biodegradable hydrogels are characteristically soft materials and it has been used in multiple biomedical applications including drug delivery carriers (Xu et al. 2018). Biodegradable hydrogel can be prepared from both natural and synthetic polymers. The use of natural polymers in the preparation of biodegradable hydrogels would be beneficial, since many natural polymers are inherently biodegradable and possess special properties, such as self-assembly, specific recognition of other molecules, and the formation of reversible bonds (Petrak 1990). Moreover, enzymatically degradable natural (alginate) hydrogel systems are to deliver endothelial progenitor cells for potential revasculature applications (Campbell et al. 2018). The oral delivery of hydrogel provides a platform for achieving maximum pharmacokinetics, tumor site-responsive controlled release, and reduced dosing of incorporated drugs (Zhang et al. 2002). Furthermore, a controlled release of intended drugs into cells and tissues means less toxicity (Himri and Guaadaoui 2018). Following this approach, formulation of pH-sensitive Zein-*co*-acrylic acid hydrogel incorporated with 5-Fu and Ru was designed to evaluate the efficiency of anticancer activity in breast cancer cells. The observed results recommend that the oral administration of formulated 5-Fu and Ru-loaded Zein-*co*-acrylic acid hydrogel exhibits its biocompatibility, constant, and controlled release and

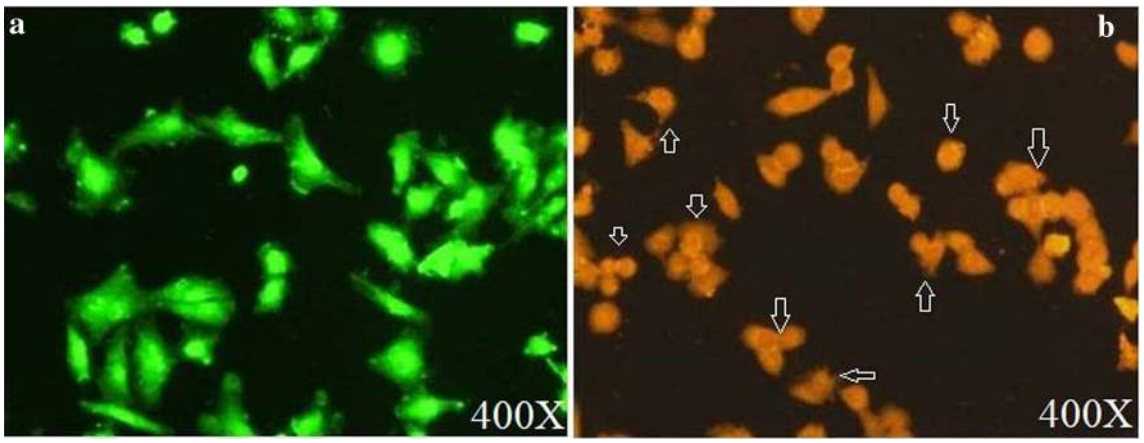

Fig. 11 Apoptosis in MDA-MB-231 cells before (**a**) and after (**b**) the treatment with 52.50 µg mL^{-1} of 5-Fu and Ru-loaded hydrogel confirmed by AO/EB staining. Irregular shape with condensed nuclei is shown with arrow

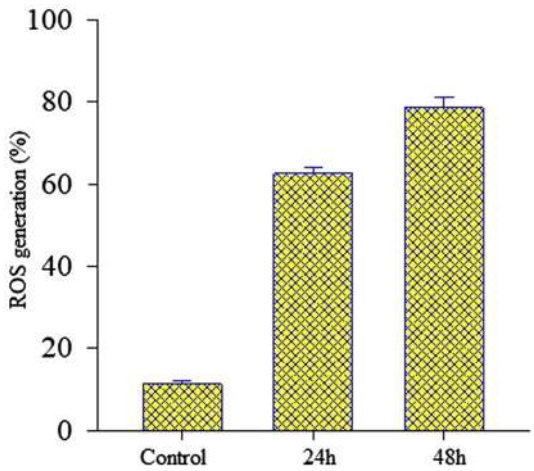

Fig. 12 Effects of 52.50 µg mL^{-1} of 5-Fu and Ru-loaded hydrogel on ROS generation (percentage of control value) in MCF-7 cancer cells. Results expressed as mean ± standard deviation triplicate measurements ($P < 0.05$)

reduced the dosage of incorporated drugs with lower toxic side effects. The dual-drug combination of natural antioxidant (Ru) along with well-known cancer drug (5-Fu) carried by the hydrogel networked vehicles, therefore, proved to be inducing antiproliferative and apoptotic effects of Ru flavonoids. In addition, it also proved its efficacy in enhancing the anticancer effects against breast cancer cells which were found to be very effective. Furthermore, the result indicated that 52.5 µg mL^{-1} of 5-Fu and Ru-loaded hydrogel showed 50% (IC_{50}) of cancer cell death.

In the present study, the graft polymerization technique was successfully applied for preparation of hydrogels, and effective characteristics of hydrogels were optimized through response surface methodology. The modeling approach of this study enabled the hybrid hydrogel formulation, drug loading, releasing studies, and ensured the optimized hydrogels impact on relevant cancer cells through swelling equilibrium method. The efficiency and efficacy of the intended cell death is mainly depending on the maximum amounts of drugs (5-Fu and Ru) loading and encapsulation. This could be identified based on optimal amount of cross-linking, and thereby increasing the amount of polymer (Zein) and monomer (acrylic acid) in the hydrogel.

There are several properties which control the rate of chemotherapeutic drugs loading and releasing from hydrogels namely pH, drug encapsulation, intrinsic viscosity, dynamic swelling, diffusion coefficient, sol–gel fraction, porosity, etc., (Wong and Dodou 2017). The pH is one of the key parameters for oral administration of hydrogels (Sharpe et al. 2014). The pH-sensitive hydrogels can be formulated through polymers with ionizable chemical groups that can accept or donate the protons. This ionizable chemical group undergoes pH-dependent changes in response to surrounding pH variation or on polymeric systems with acid-sensitive bonds. Cleavage of these acid-sensitive bonds allows release of the incorporated drugs (Kanamala et al. 2016). In our study, the –OH and $–NH_2$ group of Zein bonding with carboxyl group of acrylic acid monomer formed a weak acid-sensitive amide and carboxylic bond in the prepared hydrogel. The sensitive bond cleaved by hydrolysis and released the incorporated drugs. Furthermore, the intrinsic viscosity measurement is one of the most frequently used approaches for characterizing polymeric hydrogel molecular weight. It reflects the hydrogels melting point, crystallinity, and tensile strength in solution (Ahmed 2015). The molecular weight also produces impact on the degree of cross-linking between polymer molecules and influencing the resulting modulus (Wong et al. 2015). From the study, it was observed that the concentration of graft copolymer in the dispersion increased the intrinsic viscosity significantly. This may be achieved

to the unfolding of macromolecular chains (Zein) due to high charge density of acrylic acid monomer. The part of pH of the swelling medium of the acidic component of the polymer is an important factor in determining the swelling ratio of the hydrogels. The reason behind the above one is change in pH of the swelling medium which often leads to variations in free volumes accessible to penetrant water molecules. This ultimately affects swelling properties of the polymer (Lee and Bucknall 2008). Thus, swelling ratio of hydrogels could be dependent upon the amount of amino groups and carboxylic acids present in the hydrogel formulation. From the study, it was found the presence of less number of amino groups bringing down the swelling ratio (Yu and Xiao 2008). It is reported that the concentration of cross-linker increased the cross-linking which results in high cross-link density and thereby decreasing the water absorbency of hydrogels (Hennink and van Nostrum 2012). In the present study, the optimized Zein-*co*-acrylic acid hydrogel showed maximum equilibrium swelling ratio of 2.55 at pH 1.2 in 2 h. It is reported that swelling of the hydrogels leads to exposure of greater surface area to drug molecules which will provide penetrative and predicament impact for the drugs with the polymers.

Drug release from the cross-linked hydrogels usually takes place by a diffusion mechanism (Varshosaz and Hajian 2004). Diffusion involves migration of water or water–solvent mixtures into pre-existing of dynamically formed spaces between hydrogel chains (Üzüm and Karadağ 2010). In general, the combination of synthetic and natural polymers in hydrogel could reduce the fast entry of water and subsequently diffusion of drug out of gel structure (Biswas et al. 2016). In addition, it will retain the gel structure for a longer period of time and thereby controlling the drug release (Nayak et al. 2010). From the result in Table 3, it was observed that increase in diffusion coefficient with decreased concentration of cross-linking agent (*N*, *N*-methylene bisacrylamide) due to decrease in swelling of hydrogels. It is reported that, in sol–gel fractions of hydrogel formulation, the gel fraction increased with increasing concentration of polymer, monomer and cross-linker. The optimized hydrogel of 41–59% sol–gel fractions indicated a lower concentration of cross-linker. Furthermore, the lower amount of cross-linking in the hydrogel leads to absorbing more amount of water and retaining the capacity. The obtained results clearly indicated that the formulated hydrogel could control the release of the incorporated chemotherapeutics in oral administration. The % porosity measurements are depending on the volume of pores present in the hydrogel formulation (Barrett et al. 1951). We noticed that porosity of the hydrogel increased as the Zein and acrylic acid concentrations increased, and decreased with increasing the concentration of cross-linker. The water absorption capacity of the hydrogel is connected with distribution patterns of pores present in the polymeric structure, which further influence the mechanical properties of the hydrogel. The interconnected pores allowed the hydrogel to hold more water by capillary force (Table 4).

Physical and chemical characteristics of the unloaded hydrogel and 5-Fu and Ru-loaded hydrogel were confirmed using FTIR, XRD, SEM-EDAX, and DSC. The FTIR, a powerful technique confirmed the copolymerization reaction and cross-linking between Zein, acrylic acid, and *N*, *N*-methylene bisacrylamide. The two important peaks at 1680 cm^{-1} and 1490 cm^{-1} indicated the copolymerization between amino group of Zein and carboxylic group of acrylic acid. Furthermore, 5-Fu and Ru-loaded hydrogel spectra depict the confirmation of all peaks of drugs and pure hydrogel. It is clearly indicating that dual drugs are loaded with no interactions between hydrogel. SEM investigation showed the pores architecture surrounded inside the hydrogel. The pores structure might be due to interaction between cationic group of Zein and anionic group of acrylic acid monomer. Furthermore, the SEM images of 5-Fu and Ru-loaded hydrogel clearly showed that dual drugs uniformly distributed. In evaluation with the pure hydrogel, the hydrogel loaded with dual drugs showed a compressed structure. This was achieved by filling of pores with the drugs and the removal of the solvent from the hydrogel when it was dried after swelling. X-ray diffraction analysis confirmed the physical nature of hydrogels. In the present study, two broad peaks were observed at $2\theta = 4°$ and 16°, which corresponds to the amorphous nature of the pure and dual drug-loaded hydrogels. The thermal stability is an important characteristic of polymer material that could have biological application, considering the possible need of sterilization by heating. Thermal stability of hydrogels is depending on the cross-linking of the hydrogel.

As the aim for controlled release with less toxic, and maximizing the anticancer effect, we used a combination of natural antioxidant (Ru) with well-established anticancer drug (5-Fu) for breast cancer treatment. In general, anticancer drugs and natural antioxidants are very different in terms of structure and function. Antioxidants can synergistically maximize the effect of anticancer drugs and make them 10- to 15-fold more effective than monotherapy (Cao et al. 2016). It is reported that the soy isoflavone and daidzein improved the efficacy of tamoxifen against mammary tumors (Kwon 2014). Furthermore, the controlled release mechanism, and the physical and chemical properties of the system are carefully modified to achieve the drug release kinetics. The drug release from hydrogel will be controlled through several factors, such as (a) penetration of liquid medium into hydrogel (pores); (b) pores filled with liquid medium; (c) diffusion of the drugs in the hydrogel degradation in the fluids; (d) swelling of hydrogel; (e) the size of the drug molecules; and (f) the nature of interactions of the drug with the

Table 4 5-Fu and Ru rate release kinetics

Model	Parameter	Drug release from hydrogel			
		5-Fu at pH 1.2	Ru at pH 1.2	5-Fu at pH 7.4	Ru at pH 7.4
Zero order $F = K_0 \times t$	K_0	0.343	0.312	0.405	0.347
	r^2 adjusted	0.8703	0.9441	0.834	0.8303
	AIC	58.4938	50.5821	63.8171	61.2646
First order $F = 100 \times [1 - \mathrm{Exp}(-k_1 \times t)]$	K_1	0.006	0.005	0.007	0.006
	r^2 adjusted	0.9807	0.9818	0.9695	0.968
	AIC	41.3408	40.4832	48.5719	46.2562
Higuchi model $F = K_H \times t_{1/2}$	K_2	4.489	4.034	5.305	4.548
	r^2 adjusted	0.9523	0.9147	0.9357	0.9372
	AIC	49.4844	54.3883	55.2872	52.3171
Korsmeyer–Peppas model $F = k_{KP} \times t_n$	k_{KP}	2.189	1.096	2.81	2.446
	r^2 adjusted	0.9805	0.9818	0.9585	0.9593
	n	0.642	0.758	0.626	0.623
	AIC	43.4613	42.4581	53.3421	50.4105
Hixon–Crowell model $F = 100 \times [1 - (1 - k_{HC} \times t)3]$	k_{HC}	0.002	0.001	0.002	0.002
	r^2 adjusted	0.965	0.9809	0.9598	0.9462
	AIC	46.7121	40.8944	51.0654	50.9210

AIC akaike information criterion, F fraction of drug release in time t, K_0 apparent rate constant of zero-order release constant, K_1 first-order release constant, K_H Higuchi constant, k_{KP} Korsmeyer–Peppas rate constant, k_{HC} Hixon–Crowell constant, n diffusional exponent. And r^2 = squared correlation coefficient

polymer chains that make up the hydrogel network (Bettini et al. 1994). The interactions between drugs and hydrogels are determined based on its respective functional groups of drugs and polymers (Gupta et al. 2002). Furthermore, the drug release profile from hydrogel also depends on the pH of the releasing medium. In the present study, 5-Fu and Ru released from hydrogel are increased with increase in pH of the medium. In addition, drug release results are also coincided with swelling properties of hydrogel. This lower release of drugs at pH 1.2 is due to the protonation of carboxylate ions of Zein and acrylic acid. The protonation of carboxylate ion impacts shrinkage of the Zein-*co*-acrylic acid hydrogel which resulted in low swelling. The drug release kinetics was found to follow zero-order kinetics and non-Fickian diffusion kinetics with $n > 0.5$ for further release at higher pH.

The importance of pH-sensitive hydrogels as anticancer therapeutic vector for controlled and targeted release using in vitro cytotoxic effect on breast cancer cells (MDA-MB-231 and MCF-7) could be an enabling factor as observed. The observed inhibitory effects clearly proved that the formulated 5-Fu and Ru-loaded hydrogel could enhance the anticancer activity against breast cancer cells. Furthermore, 5-Fu and Ru-loaded hydrogel exhibited measurable cytotoxic effect against cancer cells in a dose-dependent manner. Recent report highlights that pH-sensitive hydrogels can be used as agents to avoid intracellular barrier. The pH-sensitive release behavior of 5-Fu and Ru from hydrogels is a prime factor for anticancer therapeutics. The reason behind is that most cancer tissues show relatively lower extracellular pH (~ pH 5.7–7.8) than the pH of normal tissues and blood stream. These pH variations can be easily attainable for controlled release of drugs in the specific tumor sites and reduced undesirable drug release in normal healthy tissues. Furthermore, enhanced permeation and retention (EPR) effect of pH-dependent release of 5-Fu and Ru from hydrogels will improve the release of drug to leaky blood vessels of tumor cells, as well. Moreover, the combination of Ru with 5-Fu exhibited synergistic/additive effect as anticancer/antioxidant against breast cancer cell lines in cancer therapy. Ming-Thau Sheu et al. reported that the combined effects of Doxorubicin with antioxidants (resveratrol, tetrahydroxystilbene glucoside, and curcumin) produce limited intracellular damage and causing synergistic anticancer effects (Sheu et al. 2015). More importantly, in vitro cancer cell death studies further confirmed that 5-Fu and Ru-loaded hydrogels achieved apoptosis. However, further in vivo studies may provide an elaborated view of pharmakinetics and cellular response for the formulated 5-Fu and Ru-loaded hydrogels.

Conclusions

The projected pH-sensitive hydrogels formulations are prepared using various ratios of natural polymer (Zein) with synthetic monomer (acrylic acid), as well as cross-linking

agent (*N*, *N*-methylene bisacrylamide). Well-established graft polymerization technique is used for preparation and most suitable hydrogel formulation was selected via optimization method using response surface methodology. The prepared hydrogel can be used for 5-Fu and Ru loading and delivery. Furthermore, 5-Fu and Ru-release rate kinetics was monitored through zero-order, first-order, Higuchi, Korsmeyer–Peppas, and Hixon–Crowell models. The obtained results indicated that incorporated drugs were constant and had a controlled release in a diseased site. The pH-sensitive hybrid hydrogels effectively carried the dual drugs (5-Fu and Ru) for the oral delivery with enhanced anticancer activity against breast cancer cells. Furthermore, pH-responsive hydrogels deliver drugs in and around the tumor site with enhanced cytotoxic effects and least toxic effects of normal cells/tissues. The addition of antioxidant (Ru) in the formulation has significantly reduced the dose of 5-Fu and enhanced the anticancer/antioxidant activity against breast cancer cells. In addition, 5-Fu and Ru-loaded hydrogels mediate induction of apoptosis by cancer cells due to oxidative stress in mitochondrial membrane. Altogether, the observed results suggested that the modeling approach enabled the optimized hydrogels formulation, a promising vector for oral drug delivery system.

Acknowledgements The authors are grateful to Chancellor, Vice-President, and Vice-chancellor of Kalasalingam Academy of Research and Education (Deemed to be University), Krishnankoil, India, for research fellowships and utilizing research facilities. We thank Mr. P. Kathirvel, Mr. V. Krishnaprabhu Technicians for FTIR, SEM, XRD analysis, Sir CV Raman-KS Krishnan International Research Center, Kalasalingam Academy of Research and Education (Deemed to be University), Krishnankoil, India. We also thank Prof. Z. Maciej Gliwicz, Ms. Ewa Babkiwicz, and Dr. Piotr Maszczyk, Department of Hydrobiology, Faculty of Biology, University of Warsaw, Warszawa, Poland, for timely help and support.

Author contributions SK, PT, SB, and BS designed research; SK, SB, PP, GS, JN, and AW performed research; SM, SA, and BS contributed new reagents or analytical tools. All authors read and approved the final manuscript.

Compliance with ethical standards

Conflict of interest The authors report no financial interest that might pose a potential, perceived, or real conflict of interest. The authors declare there are no competing interests.

References

Ahmed EM (2015) Hydrogel: preparation, characterization, and applications: a review. J Adv Res 6(2):105–121

Alberts B, Johnson A, Lewis J, Raff M, Roberts K, Walter P (2002) Cancer treatment: present and future. In: Molecular biology of the cell, 4th edn. Oxford University Press, Garland Science, New York

Alla SGA, El-Din HMN, El-Naggar AWM (2007) Structure and swelling-release behaviour of poly (vinyl pyrrolidone) (PVP) and acrylic acid (AAc) copolymer hydrogels prepared by gamma irradiation. Eur Polymer J 43(7):2987–2998

Arıca B, Çalış S, Kaş H, Sargon M, Hıncal A (2002) 5-Fluorouracil encapsulated alginate beads for the treatment of breast cancer. Int J Pharm 242(1–2):267–269

Aydin R, Pulat M (2012) 5-Fluorouracil encapsulated chitosan nanoparticles for pH-stimulated drug delivery: evaluation of controlled release kinetics. J Nanomater 2012:1–10

Barrera G (2012) Oxidative stress and lipid peroxidation products in cancer progression and therapy. ISRN Oncol 2012:1–22

Barrett EP, Joyner LG, Halenda PP (1951) The determination of pore volume and area distributions in porous substances. I. Computations from nitrogen isotherms. J Am Chem Soc 73(1):373–380

Bashir S, Teo YY, Naeem S, Ramesh S, Ramesh K (2017) pH responsive *N*-succinyl chitosan/poly (acrylamide-*co*-acrylic acid) hydrogels and in vitro release of 5-fluorouracil. PLoS One 12(7):e0179250

Bastiancich C, Bozzato E, Luyten U, Danhier F, Bastiat G, Préat V (2019) Drug combination using an injectable nanomedicine hydrogel for glioblastoma treatment. Int J Pharm 548(1):522–529

Bettini R, Colombo P, Massimo G, Catellani PL, Vitali T (1994) Swelling and drug release in hydrogel matrices: polymer viscosity and matrix porosity effects. Eur J Pharm Sci 2(3):213–219

Biswas GR, Majee SB, Roy A (2016) Combination of synthetic and natural polymers in hydrogel: an impact on drug permeation. J Appl Pharm Sci 6(11):158–164

Brazel CS, Peppas NA (1995) Synthesis and Characterization of thermo-and chemomechanically responsive poly (*N*-isopropylacrylamide-*co*-methacrylic acid) hydrogels. Macromolecules 28(24):8016–8020

Calabro M, Tommasini S, Donato P, Stancanelli R, Raneri D, Catania S, Costa C, Villari V, Ficarra P, Ficarra R (2005) The rutin/β-cyclodextrin interactions in fully aqueous solution: spectroscopic studies and biological assays. J Pharm Biomed Anal 36(5):1019–1027

Caló E, Khutoryanskiy VV (2015) Biomedical applications of hydrogels: a review of patents and commercial products. Eur Polymer J 65:252–267

Campbell KT, Stilhano RS, Silva EA (2018) Enzymatically degradable alginate hydrogel systems to deliver endothelial progenitor cells for potential revasculature applications. Biomaterials 179:109–121

Cao J, Han J, Xiao H, Qiao J, Han M (2016) Effect of tea polyphenol compounds on anticancer drugs in terms of anti-tumor activity, toxicology, and pharmacokinetics. Nutrients 8(12):762

Carmeliet P, Jain RK (2000) Angiogenesis in cancer and other diseases. Nature 407(6801):249

Da Costa CAM, Moraes ÂM (2003) Encapsulation of 5-fluorouracil in liposomes for topical administration. Maringá 25(1):53–61

Dai X, Tan C (2015) Combination of microRNA therapeutics with small-molecule anticancer drugs: mechanism of action and co-delivery nanocarriers. Adv Drug Deliv Rev 81:184–197

Damaraju VL, Damaraju S, Young JD, Baldwin SA, Mackey J, Sawyer MB, Cass CE (2003) Nucleoside anticancer drugs: the role of nucleoside transporters in resistance to cancer chemotherapy. Oncogene 22(47):7524

Danhier F, Feron O, Préat V (2010) To exploit the tumor microenvironment: passive and active tumor targeting of nanocarriers for anti-cancer drug delivery. J Control Release 148(2):135–146

Djeridane A, Yousfi M, Nadjemi B, Boutassouna D, Stocker P, Vidal N (2006) Antioxidant activity of some Algerian medicinal plants extracts containing phenolic compounds. Food Chem 97(4):654–660

Eng C (2009) Toxic effects and their management: daily clinical challenges in the treatment of colorectal cancer. Nat Rev Clin Oncol 6(4):207–218

Ferlay J, Shin HR, Bray F, Forman D, Mathers C, Parkin DM (2010) Estimates of worldwide burden of cancer in 2008: GLOBOCAN 2008. Int J Cancer 127(12):2893–2917

Florea A-M, Büsselberg D (2011) Cisplatin as an anti-tumor drug: cellular mechanisms of activity, drug resistance and induced side effects. Cancers 3(1):1351–1371

Gil ES, Hudson SM (2004) Stimuli-reponsive polymers and their bioconjugates. Prog Polym Sci 29(12):1173–1222

Gupta P, Vermani K, Garg S (2002) Hydrogels: from controlled release to pH-responsive drug delivery. Drug Discov Today 7(10):569–579

Hennink WE, van Nostrum CF (2012) Novel crosslinking methods to design hydrogels. Adv Drug Deliv Rev 64:223–236

Hickey T, Kreutzer D, Burgess D, Moussy F (2002) Dexamethasone/PLGA microspheres for continuous delivery of an anti-inflammatory drug for implantable medical devices. Biomaterials 23(7):1649–1656

Himri I, Guaadaoui A (2018) Cell and organ drug targeting: types of drug delivery systems and advanced targeting strategies. In: Nanostructures for the engineering of cells, tissues and organs. William Andrew, Elsevier, Oxford, pp 1–66

Hoffman A (1998) Pharmacodynamic aspects of sustained release preparations. Adv Drug Deliv Rev 33(3):185–199

Johnstone RW, Ruefli AA, Lowe SW (2002) Apoptosis: a link between cancer genetics and chemotherapy. Cell 108(2):153–164

Kanamala M, Wilson WR, Yang M, Palmer BD, Wu Z (2016) Mechanisms and biomaterials in pH-responsive tumour targeted drug delivery: a review. Biomaterials 85:152–167

Kevadiya BD, Joshi GV, Mody HM, Bajaj HC (2011) Biopolymer–clay hydrogel composites as drug carrier: host–guest intercalation and in vitro release study of lidocaine hydrochloride. Appl Clay Sci 52(4):364–367

Kumari A, Yadav SK, Yadav SC (2010) Biodegradable polymeric nanoparticles based drug delivery systems. Colloids Surf B 75(1):1–18

Kunjiappan S, Panneerselvam T, Somasundaram B, Sankaranarayanan M, Chowdhury R, Chowdhury A, Bhattacharjee C (2018) Design, in silico modeling, biodistribution study of rutin and quercetin loaded stable human hair keratin nanoparticles intended for anticancer drug delivery. Biomed Phys Eng Express 4(2):025019

Kwon Y (2014) Effect of soy isoflavones on the growth of human breast tumors: findings from preclinical studies. Food Sci Nutr 2(6):613–622

Labib G (2018) Overview on Zein Protein: a promising pharmaceutical excipient in drug delivery systems and tissue engineering. Expert Opin Drug Deliv 15(1):65–75

Langer R, Peppas NA (1981) Present and future applications of biomaterials in controlled drug delivery systems. Biomaterials 2(4):201–214

Lee JH, Bucknall DG (2008) Swelling behavior and network structure of hydrogels synthesized using controlled UV-initiated free radical polymerization. J Polym Sci Part B Polym Phys 46(14):1450–1462

Leslie A (1954) Ethics and practice of placebo therapy. The American Journal of Medicine 16(6):854–862

Lin C-C, Metters AT (2006) Hydrogels in controlled release formulations: network design and mathematical modeling. Adv Drug Deliv Rev 58(12–13):1379–1408

Lordi NG (1986) Sustained release dosage forms. Theory Pract Ind Pharm 3:430–456

Lutolf M, Hubbell J (2003) Synthesis and physicochemical characterization of end-linked poly (ethylene glycol)-*co*-peptide hydrogels formed by Michael-type addition. Biomacromol 4(3):713–722

Malafaya PB, Silva GA, Reis RL (2007) Natural–origin polymers as carriers and scaffolds for biomolecules and cell delivery in tissue engineering applications. Adv Drug Deliv Rev 59(4–5):207–233

Memic A, Alhadrami HA, Hussain MA, Aldhahri M, Al Nowaiser F, Al-Hazmi F, Oklu R, Khademhosseini A (2015) Hydrogels 2.0: improved properties with nanomaterial composites for biomedical applications. Biomed Mater 11(1):014104

Nair LS, Laurencin CT (2007) Biodegradable polymers as biomaterials. Prog Polym Sci 32(8–9):762–798

Nayak AK, Malakar J, Sen KK (2010) Gastroretentive drug delivery technologies: current approaches and future potential. J Pharm Educ Res 1(2):1–12

Ninan N, Forget A, Shastri VP, Voelcker NH, Blencowe A (2016) Antibacterial and antiinflammatory pH-responsive tannic acid-carboxylated agarose composite hydrogels for wound healing. ACS Appl Mater Interfaces 8(42):28511–28521

Omer A, Tamer T, Hassan M, Rychter P, Eldin MM, Koseva N (2016) Development of amphoteric alginate/aminated chitosan coated microbeads for oral protein delivery. Int J Biol Macromol 92:362–370

Peppas N, Bures P, Leobandung W, Ichikawa H (2000) Hydrogels in pharmaceutical formulations. Eur J Pharm Biopharm 50(1):27–46

Peters GJ, Ackland SP (1996) Leading article: oncologic, endocrine and metabolic: new antimetabolites in preclinical and clinical development. Expert Opin Investig Drugs 5(6):637–679

Petrak K (1990) Polymers for use in drug delivery—property and structure requirements. Br Polym J 22(3):213–219

Ps S, Joshi VG (2013) Preparation and characterisation of 5-fluorouracil loaded PLGA nanoparticles for colorectal cancer therapy. Unique J Pharm Biol Sci 01(02):52–58

Rama AR, Hernandez R, Perazzoli G, Burgos M, Melguizo C, Vélez C, Prados J (2015) Specific colon cancer cell cytotoxicity induced by bacteriophage E gene expression under transcriptional control of carcinoembryonic antigen promoter. Int J Mol Sci 16(6):12601–12615

Ramalingam V, Varunkumar K, Ravikumar V, Rajaram R (2016) Development of glycolipid biosurfactant for inducing apoptosis in HeLa cells. RSC Adv 6(68):64087–64096

Ranjha NM, Qureshi UF (2014) Preparation and characterization of crosslinked acrylic acid/hydroxypropyl methyl cellulose hydrogels for drug delivery. Int J Pharm Pharm Sci 6(4):400–410

Ranjha NM, Ayub G, Naseem S, Ansari MT (2010) Preparation and characterization of hybrid pH-sensitive hydrogels of chitosan-*co*-acrylic acid for controlled release of verapamil. J Mater Sci Mater Med 21(10):2805–2816

Ryu J-H, Chacko RT, Jiwpanich S, Bickerton S, Babu RP, Thayumanavan S (2010) Self-cross-linked polymer nanogels: a versatile nanoscopic drug delivery platform. J Am Chem Soc 132(48):17227–17235

Sahoo S, Chung C, Khetan S, Burdick JA (2008) Hydrolytically degradable hyaluronic acid hydrogels with controlled temporal structures. Biomacromol 9(4):1088–1092

Sakamoto JH, van de Ven AL, Godin B, Blanco E, Serda RE, Grattoni A, Ziemys A, Bouamrani A, Hu T, Ranganathan SI (2010) Enabling individualized therapy through nanotechnology. Pharmacol Res 62(2):57–89

Schmaljohann D (2006) Thermo-and pH-responsive polymers in drug delivery. Adv Drug Deliv Rev 58(15):1655–1670

Selvaraj K, Chowdhury R, Bhattacharjee C (2013) Isolation and structural elucidation of flavonoids from aquatic fern *Azolla microphylla* and evaluation of free radical scavenging activity. Int J Pharm Pharm Sci 5(3):743–749

Selvaraj K, Chowdhury R, Bhattacharjee C (2014) Optimization of the solvent extraction of bioactive polyphenolic compounds from aquatic fern *Azolla microphylla* using response surface methodology. Int Food Res J 21(4):1559–1567

Sharpe LA, Daily AM, Horava SD, Peppas NA (2014) Therapeutic applications of hydrogels in oral drug delivery. Expert Opin Drug Deliv 11(6):901–915

Sheu M-T, Jhan H-J, Hsieh C-M, Wang C-J, Ho H-O (2015) Efficacy of antioxidants as a complementary and alternative medicine (CAM) in combination with the chemotherapeutic agent doxorubicin. Integr Cancer Ther 14(2):184–195

Siegel RL, Miller KD, Jemal A (2019) Cancer statistics, 2019. CA Cancer J Clin 69(1):7–34

Trachootham D, Alexandre J, Huang P (2009) Targeting cancer cells by ROS-mediated mechanisms: a radical therapeutic approach? Nat Rev Drug Discov 8(7):579–591

Üzüm ÖB, Karadağ E (2010) Equilibrium swelling studies of chemically cross-linked highly swollen acrylamide-sodium acrylate hydrogels in various water-solvent mixtures. Polym Plast Technol Eng 49(6):609–616

Varshosaz J, Hajian M (2004) Characterization of drug release and diffusion mechanism through hydroxyethylmethacrylate/methacrylic acid pH-sensitive hydrogel. Drug Deliv 11(1):53–58

Viloria-Petit A, Crombet T, Jothy S, Hicklin D, Bohlen P, Schlaeppi JM, Rak J, Kerbel RS (2001) Acquired resistance to the antitumor effect of epidermal growth factor receptor-blocking antibodies in vivo: a role for altered tumor angiogenesis. Can Res 61(13):5090–5101

Wong RSH, Dodou K (2017) Effect of drug loading method and drug physicochemical properties on the material and drug release properties of poly (ethylene oxide) hydrogels for transdermal delivery. Polymers 9(7):286–315

Wong RSH, Ashton M, Dodou K (2015) Effect of crosslinking agent concentration on the properties of unmedicated hydrogels. Pharmaceutics 7(3):305–319

Xu L, Qiu L, Sheng Y, Sun Y, Deng L, Li X, Bradley M, Zhang R (2018) Biodegradable pH-responsive hydrogels for controlled dual-drug release. J Mater Chem B 6(3):510–517

Yahia L, Chirani N, Gritsch L, Motta FL, Fare S (2015) History and applications of hydrogels. J Biomed Sci 4(2):1–13

Yin L, Fei L, Cui F, Tang C, Yin C (2007) Superporous hydrogels containing poly (acrylic acid-*co*-acrylamide)/*O*-carboxymethyl chitosan interpenetrating polymer networks. Biomaterials 28(6):1258–1266

Yu H, Xiao C (2008) Synthesis and properties of novel hydrogels from oxidized konjac glucomannan crosslinked gelatin for in vitro drug delivery. Carbohyd Polym 72(3):479–489

Zhang X-Z, Zhuo R-X, Cui J-Z, Zhang J-T (2002) A novel thermoresponsive drug delivery system with positive controlled release. Int J Pharm 235(1–2):43–50

Zohuriaan-Mehr MJ, Kabiri K (2008) Superabsorbent polymer materials: a review. Iran Polym J 17(6):451